STUDY AND IMPLEMENTATION OF OBSTACLE DETECTION AND AVOIDANCE USING SONAR

BY

MAYERO CHRISTOPHER

A THESIS SUBMITTED IN PARTIAL FULFILLMENT OF THE REQUIREMENTS FOR THE DEGREE OF MASTER OF SCIENCE IN EXPERIMENTAL PHYSICS

FACULTY OF SCIENCE

MASENO UNIVERSITY

© 2012

ABSTRACT

In robotics research, ensuring that robotic systems accurately detect and avoid both static and moving objects is the main challenge to building robots more autonomous. This thesis presents a method of accurately obtaining the position of an obstacle from a robot system by considering the angular orientation of the obstacle in an indoor unstructured or structured environment. The method used is an advanced sonar sensing method that overcomes the problem of conventional ultrasonic ranging that provides the direction of the reflecting point. Conventional ultrasonic sensors do not provide the reflecting point accurately, therefore, inconvenient to use in detecting obstacles where accuracy in range measurement is required. The method described in this thesis was implemented and tested on a physical robot. The robot, named Polyrobot, has two ultrasonic transducers at extreme ends of the robot's front panel at a fixed distance. The robot used was fully autonomous with all power and processing onboard. The robot was programmed in wiring language (Arduino C version 11). All experimental data were gathered in unaltered indoor laboratory environment with both static and dynamic obstacles. The ultrasonic transducers were used to measure distance between the robot and obstacles, with the distance between the two transducers taken as the constant obstacle width. The range measurements from the two transducers were uploaded to the microcontroller board on the robot and displayed on personal computer monitor. Logic functions using comparison operators were developed based on the range measurements at different obstacle angular position with reference to robot centre and incorporated in the algorithm using the Arduino C version 11. The logic functions in the algorithm are responsible for decision making, enabling the robot to make decisions on whether to move forward, turn right, turn left, stop or reverse in order to avoid an obstacle. The data from the sonar sensors were used as the input variables. The output variables were the curvatures (turns) and velocity of the robot wheel motors (actuators) in order to avoid an obstacle. The developed algorithm is the artificial

v

CHAPTER ONE

INTRODUCTION

Obstacle avoidance, also known as reflexive obstacle avoidance (or local path planning) is one of the key issues to successful application of mobile robot system. The process is divided into obstacle detection and avoidance control. Mobile robots feature some kind of collision avoidance ranging from basic algorithms that detect an obstacle and stop the robot in order to avoid collision, through more advanced algorithms, that enable the robot to detour the obstacle. The latter algorithms are much more complex since they involve not only the detection of obstacle, but also some kind of quantitative measurements concerning the dimensions of obstacle. Once these measurements have been determined, the obstacle avoidance algorithm needs to steer the robot around the obstacle and proceed towards the original target. Usually, the procedure requires the robot to stop in front of the obstacle, take measurements with the aid of sensor system used, after which, it resumes motion.

An autonomous mobile robot is defined by the American Robot Institute as "a programmable, multifunctional manipulator designed to move material parts, tools or specialized devices through various programmed motion for performance of a variety of tasks"[1]. It is therefore a sophisticated, computer controlled intelligent system. The major components of an advanced robot system are: vision guidance, steering control, obstacle avoidance, speed control, safety and braking, power unit and a supervisor control PC. The adaptive capabilities of a mobile robot depend on fundamental analytical and architectural designs of sensor system used.

Robot design generally falls into two categories: fixed industrial robots and mobile robots [2, 3]. UGVs are a group of mobile robots which fall in the second category and have great promising potential for the future. Areas that traditionally have been emphasized and the laboratory results are beginning to find

1

applications in the real world are space exploration [4, 5], material handling [6] and transportation, medical transport of food and patients and future combat vehicles [7].

The more complex a robot's working place gets, the more sophisticated its obstacle detection and avoidance facilities need to be designed. First, the sensor equipment must be appropriate for the requirements of the given scenarios. In most cases such sensors have a limited field of vision and therefore cannot cover the complete area around the robot. One possibility to overcome this limitation is mounting several such sensors on the robot system. In animals, for example mammals, the short-term memory is used to compensate for the relatively small field of vision. As an example, the hind legs of a cat have to avoid obstacles some time after the cat has visually perceived the hindrance [8]. Clearly the cat has to keep in mind certain information about its local environment in order to safely navigate complex terrain. In this work, an approach for adopting the principle of short-term obstacle memory for mobile indoor robots is provided by a buffer in the sensor system used (LV-Max Sonar-EZ1) that holds the previous output until new output is available, thus the determining factor of how often to store values is the reaction time of the robot to avoid obstacles.

Robots require a wide range of sensors to obtain information about the world around them (world modeling). This is what provides raw data to develop the basic mathematical and geometrical relationships between the robot and the obstacles. The raw data include, distance, width of obstacle, shape of obstacle and angular orientation of obstacle. Knowing the shape, or class, of a target assists in robot localization and mapping applications. It enables prediction of how the target will appear from different sensor positions, and simplifies associating environmental features to a map. Mistakes in associating environmental features to a map can lead to persistent gross errors in range measurements. Knowing the width of the obstacle is an important parameter for finding the path of the robot to avoid an obstacle while the distance from the obstacle, provides the minimum

2

safe distance for the robot to start making decisions. The latter is based on the navigation rules setup in the navigation algorithm. The robot will then make a decision to turn left, or right, or go straight, or stop, or reverse.

1.1 Background of study

1.1.1 Sonar Sensing

Sonar sensing fulfills the requirements of intelligent, fast, accurate, reliable and cheap sensors as required in robotics research. Moreover sonar physics provides robotics researchers with a natural selection capability for landmark detection in navigation problems. Advanced sonar sensing can be addressed by examining firstly sonar that is not advanced, such as a single Polaroid Ranging Module (PRM) [9]. In its commonly applied form, PRM supplies a range estimate derived from thresholding the first echo out to a maximum range of 10 meters. The beam width depends on range and target reflectivity. Very little information about the target, the angle to the target, the strength of the echo or whether the echo comes from the sonar system or another is obtained from such a system. Advanced sonar can accurately determine angle, target classification, target strength, multiple targets and whether that sonar system owns an echo, allowing rejection of interference.

Sonar is a popular sensor in robotics that employs acoustic pulses and their echoes to measure range to an obstacle. Its popularity is due to its light weight, low power consumption, low computational effort, low cost, ease of implementation, inherent safety, less affected by target material and surfaces, not affected by colour, solid state units have virtually unlimited maintenance free life, can detect small objects over long operating distances, resistance to external disturbance such as vibration, infrared radiation, ambient noise and EMI radiation, compared to other ranging sensors. Since the speed of sound is usually known, the object range is proportional to the echo travel time. At ultrasonic frequencies the sonar

3

energy is concentrated in a beam, providing directional information in addition to range.

Sonar in robotics has three different, but related purposes:

- **Obstacle avoidance**: The first detected echo is assumed to measure the range to the closest object. Robots use this information to plan paths around obstacles and to prevent collision.

- **Sonar mapping**: A collection of echoes acquired by performing a rotational scan or form a sonar array, are used to construct a map of the environment. Similar to a radar display, a range dot is placed at detected range along the probing pulse direction.

- **Object recognition**: A sequence of echoes or sonar maps are processed to classify echo producing structures composed of one or more physical objects. When successful, this information is useful for robot registration or landmark navigation [10].

Bats are mammals that have biological sonar. Bats can distinguish between objects that are just 0.3mm apart, know the size, the location, the speed, the direction of the movement and even the thickness of the insect they are hunting [11]. In this respect, they carry out collision-free activities through a cave while teeming with thousands of other bats, in total darkness or under heavy rain. These amazing abilities certainly persuade the skeptics to accept the potentialities of the ultrasonic acoustic sensors.

1.1.2 Time of Flight (TOF) and the phase difference (Phase-Shift) ranging techniques

Ultrasonic sensors used for purposes of map building involve distance measurements based on the TOF of a pulse of emitted energy travelling to a reflecting object, then echoing back to a receiver, and the phase-shift

measurement (or phase detection) ranging technique which involves continuous wave transmission as opposed to the short pulsed outputs used in TOF systems.

1.1.2.1 TOF method

In this method the measured pulses come from an ultrasonic source. The relevant parameters involved in range calculations are speed of sound in air (v) and the elapsed time (t) required to travel the round trip distance. Using elementary Physics, distance is determined by multiplying the velocity of the energy wave by the time required to travel the round-trip distance.

$$s = vt \tag{1}$$

where s is the round-trip distance, v is the speed of propagation and t is the elapsed time.

The measured time is the representative of traveling twice the separation distance and must therefore be reduced by half to result in actual range of target.

The advantage of TOF systems arises from the direct nature of their straight line active sensing. The returned signal follows essentially the same path back to a receiver located coaxially with or in close proximity to the transmitter. In fact, it is possible in some cases for the transmitting and receiving transducers to be the same device. Furthermore, TOF sensors maintain range accuracy in a linear fashion as long as reliable echo detection is sustained.

Potential error sources for TOF systems using sonar include:

1. The wide sonar beam causes a poor directional resolution. Objects are located at the middle of isolated arcs, but closer-range objects shorten the arcs of those at farther ranges, and the arcs produced by a collection of objects are often difficult to interpret. A consequence of this effect is that wide beams occlude small openings, limiting robot navigation.

3. Smooth surfaces at oblique incidence do not produce detectable echoes. Figure 1.1 shows a planar surface, a wall that acts as a mirror to the sonar beam. The important point is that the nearby wall does not itself produce a detectable echo, and a robot using sonar for obstacle avoidance may collide with the wall.
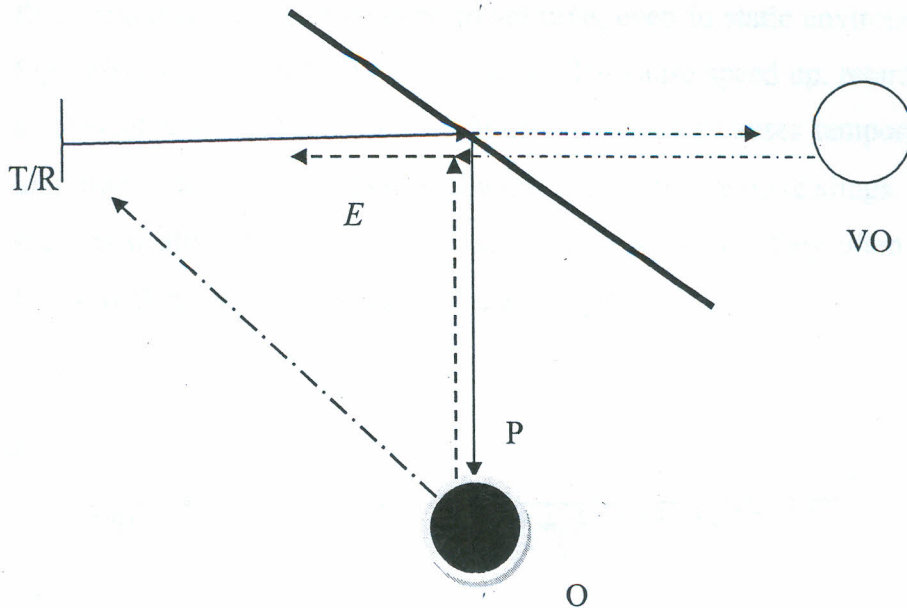
Figure 1.1   **Smooth surface redirects beam causing sonar artifact at virtual object (VO) location. Dot –dashed echo path falls outside sonar beam and does not produce detectable echo**

4. Artifacts caused by beam side lobes and multiple reflections produce range readings in the environment where no objects exist. Figure 1.1 also shows the re-directed beam enclosing object O. The echo also is redirected by the wall back to the transducer. From the transducer's reference, the object is at the virtual object location VO, and it would generate the same sonar map shown in Figure 1.0. Since there is no physical object corresponding to the sonar dot location, it is an artifact. Also, note that the

acoustic energy indicated by the dot-dashed line reflected back to the transducer is not detected because it does not lie within the beam cone. Beam side lobes often detect these echoes and produce nearer range readings but placed along the sonar orientation.

5. Travel time and amplitude variations in the echoes caused by inhomogeneities in the sound speed. Both effects cause random fluctuations in the detected echo travel time, even in static environments. Figure 1.2 illustrates thermal fluctuations that cause speed up, retardation, and travel re-direction by refraction of echoes. This causes temporal and amplitude variations in echoes including jitter in the range readings. While these typically introduce minor changes in sonar maps, they often cause havoc with approaches using finer analysis [10].
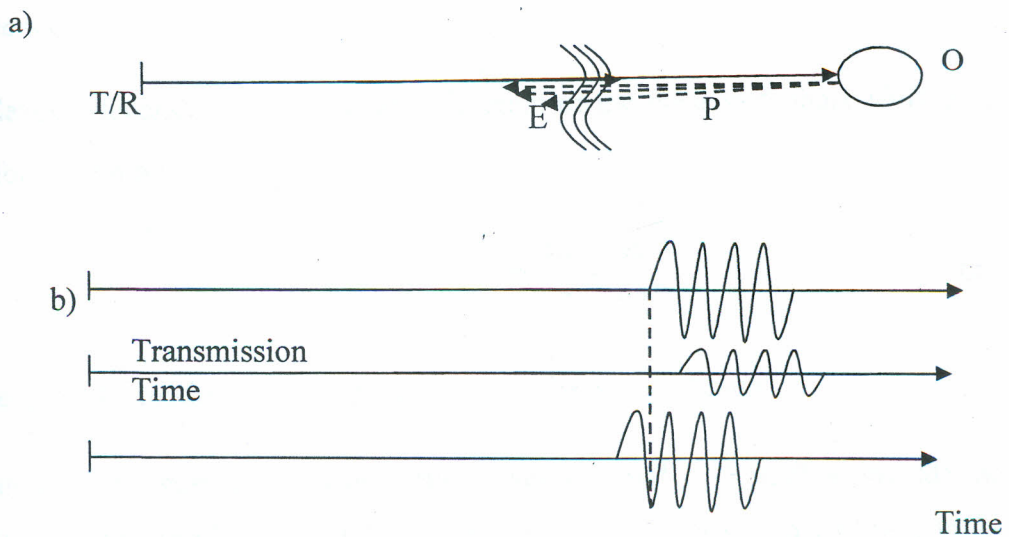
a)

b)

Transmission
Time

Time

Figure 1.2 **a, b Random echo jitters. (a) Sonar configuration. Thermal inhomogeneities in the acoustic transmission medium cause refraction effects. (b) Examples of variations in echo travel times and amplitudes in a static environment**

1.1.2.2 Phase-shift measurement of phase-detection ranging technique

This method involves continuous wave transmission as opposed to the short pulsed outputs used in TOF measurement method. A beam of amplitude modulated acoustical energy is directed towards the target. A small portion of this wave (potentially up to six orders of magnitude less in amplitude) is reflected by the objects surface back to the detector along a direct path. The returned energy is compared to a simultaneously generated reference that has a split off from the original signal, and the relative phase shift between the two is measured to ascertain the round trip distance the wave has travelled. The relative phase-shift expressed as a function of distance to the reflecting target surface is,

$$\phi = \frac{4\pi d}{\lambda} \tag{2}$$

where ϕ is the phase shift, d is the distance to target and λ is the modulation wavelength.

The desired distance to target d as a function of the measured phase shift ϕ is therefore given by

$$d = \frac{\phi\lambda}{4\pi} = \frac{\phi c}{4\pi f} \tag{3}$$

where f is the modulation frequency and c is the speed of light

Advantages of a continuous-wave system over a pulsed TOF method include the ability to measure direction and velocity of a moving target in addition to its range. As with TOF method, the paths of the source and the reflected beam are coaxial for phase-shift-measurement system. This characteristic ensures objects cannot cast shadows when illuminated by energy source, preventing the missing parts problem. Even greater measurement accuracy and overall range can be

achieved when co-operative targets are attached to the objects of interest to increase power density of the returned signal [12].
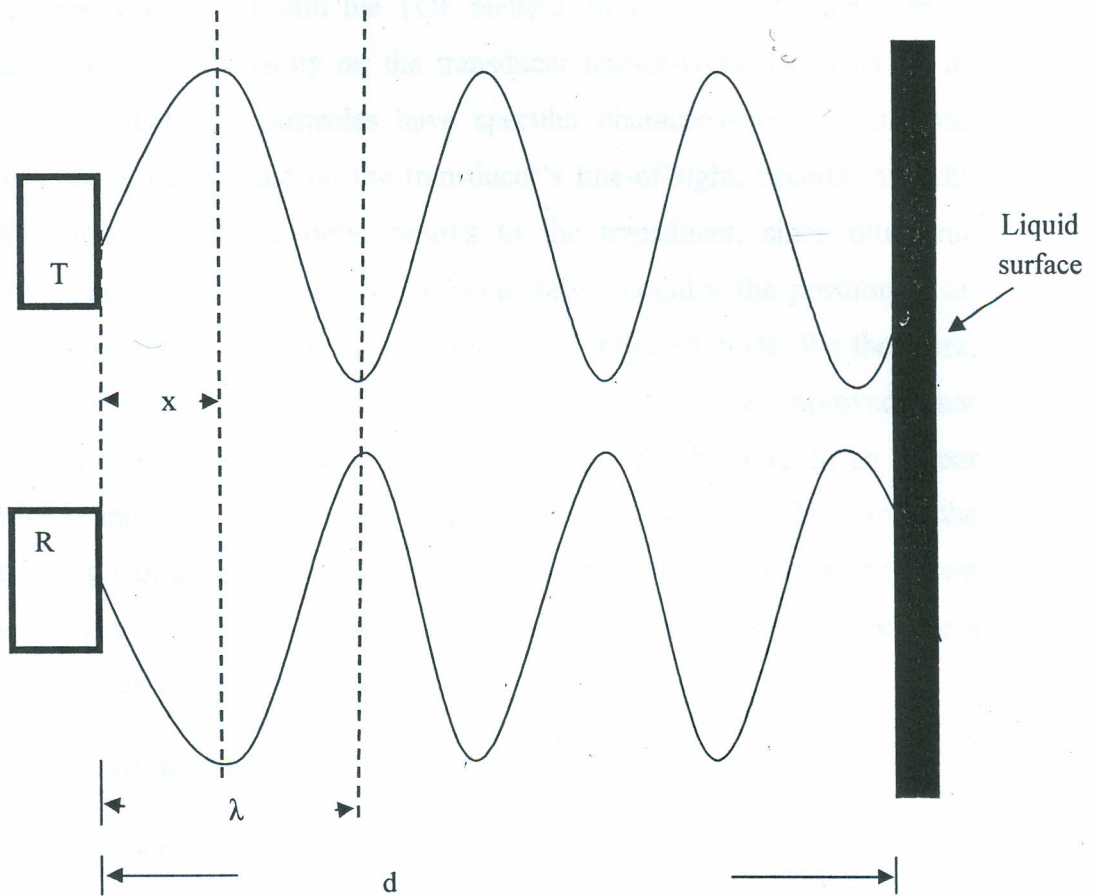

Figure 1.3 Relationship between outgoing and reflected waveforms, where x is the distance corresponding to the distance corresponding to the differential phase.

Our study is built on phase-shift measurement using multiple ultrasonic transducers. The phase-shift in this sense is computed as the difference of range readings between the left and the right ultrasonic transducers.

1.2 Statement of the problem

With a conventional ultrasonic sensor system for a mobile robot, the distance to an object can be obtained with the TOF method, in which a reflected point is regarded to be located directly on the transducer line-of-sight. However, in an indoor environment, flat obstacles have specular characteristics. So, the real reflected point is not located on the transducer's line-of-sight, because an echo from the normal incidence only, returns to the transducer, since ultrasonic directivity is not so sharp in air. So, to accurately recognize the position of an object, it is important to detect the direction of the reflected point. We therefore, improve the sonar sensing system by using two transducers. The improved sonar sensing provide range information, inclination angle of obstacles in an indoor environment and recognize precisely the reflected point. In this work the inclination angle of an obstacle is solved for using range information from the two transducers. The inclination angle is used to accurately position and navigate a robot system in an indoor environment.

1.3 Objectives of the study

The objectives of the study were to:
1. study obstacle detection considering specularities of flat surfaces in an indoor environment and
2. Obtain a method of accurately locating obstacles in an environment, in mobile robot operation based on their angular orientations.

1.4 Scope of the study

This study was limited to:

1. identifying a suitable ultrasonic sensor for effective obstacle detection while considering drawbacks of the ultrasonic ranging system,
2. identifying a suitable microcontroller,

11

3. designing a complete working circuit for interfacing robot controls (actuators), microcontroller, personal computer and ultrasonic sensors and

4. designing an intelligence algorithm required by the robot using a suitable programming language to serve as the artificial intelligence in order to make correct decisions.

1.5 Significance of the study

The results from this study can be used to improve on obstacle detection procedure in mobile robot navigation in an indoor environment where flat obstacles have specular characteristics. The decision to be made by an autonomous robot system on whether to turn left, turn right, stop, reverse, or go straight ahead in order to avoid an obstacle by considering the distance, width, shape of the obstacle and its angular orientation is more accurate due to minimized errors in range measurement. Due to the method developed in this work, accurate obstacle recognition through detection and more accurate range measurement has been realized.

CHAPTER TWO
LITERATURE REVIEW

2.1 Improved sonar sensing

Ultrasound TOF sensors normally used in mobile robot applications such as distance measurement, environment perception and robot navigation [13, 14] have been around for a while. In many applications like environment perception or robot navigation, ultrasonic sensors have been considered to be unreliable and inaccurate, due to the wide opening angle that introduces a high angular uncertainty.

On the other hand ultrasound sensors are simple in construction and use, mechanically robust, and provide a cost-effective process for environment perception. The widely used Polaroid device is inexpensive, easily integrated and has found wide use in robotic applications. Due to the importance of ultrasound sensors, much of the latest research work has been focused on the ultrasound rangefinder data interpretation and improvement [15]. Regarding data interpretation, several physical simulation models [13] and experimental based models derived from data collection [16, 14] have been addressed.

An external sensor is very important for a mobile robot to recognize its environment and its own position. In particular, the range sensor, which can measure the distance to objects, is used to recognize the physical shape of the environment. Ultrasonic transducers are preferably used to obtain three dimensional information about the environment. The most commonly used sonar device for mobile robots is the well known Polaroid ultrasonic ranging system [9] with a detection cone of 30^0.

Map construction problem with ultrasonic range sensors, has presented several solutions. Improving the sensing system by use of multiple transducers is one such approach. Recently, several research results have been published which use

13

the transducer array to form an ultrasonic beam. These include work done by Wilkes *et al.* [17] who presented an algorithm that uses multiple peaks in the return signals from several transducers with broad beams of 70^0 and overlapping fields of view; but they do not exploit cross echoes from neighbor sensors. A grid based representation and a Bayesian update scheme similar to Matthies and Elfes [18] are used to integrate the multiple return signals from multiple transducers and multiple robot positions.

A triaural measurement system that uses one transmitting and three receiving ultrasonic sensors to distinguish between planes, corners and edges by means of triangulation was proposed by Peremans and Van Campenhout [19]. They argue that by triaural sensing, much less measurements are necessary to recognize planes, corners and edges, the three basic reflector types, in comparison to standard time-of-flight sensor systems.

Lawitzky *et al.* [20] compare monaural (1 transmitter, 1 receiver), binaural (1 transmitter, 2 receivers) and triaural (1transmitter, 3 receivers) sensor system configurations. They state that binaural or triaural sensing allows getting more information from a single measurement by sensing several features at once. For this reason they conclude that these principles have a large potential for increasing speed and precision of environment mapping for obstacle avoidance and navigation.

An approach which allows the simultaneous firing of sonar sensors by eliminating misreading caused by crosstalk or external ultrasound sources was presented by J'org and Berg [21]. Simultaneous firing of sonar sensors is achieved by using appropriate pseudorandom sequences together with a matched filter technique. Polaroid series transducers are used and crosstalk can either be eliminated or can be exploited to perform triangulation.

14

Wirnitzer *et al.* [22] use stochastic coding of the transmitted signals and adaptive filtering of the received signals to avoid mutual interference of the sensors and interference with other ultrasonic sensor systems. The target application is an automotive low range detection system such as a car parking assistant where wide angled sensors are employed and cross echoes are explicitly used. An array of several sensors allows, distance measurements in addition to localizing an obstacle inside the operating range of at least two sensors of the array. Additional shape information can be obtained when the sensors operate in the cross echo mode. Based on this ultrasonic sensing system, Schmidt *et al.* [23] describe a triangulation based algorithm which allows for distinguishing between circular and plane objects and to identify obstacle edges.

However, most of this work does not consider the property of the reflection of surfaces of obstacles due to specular characteristics of surfaces of obstacles. This makes the real reflected point not to be located on the line-of-sight of the transducer, because an echo from the normal incidence only, returns to the transducer, since ultrasonic directivity is not sharp in air. Therefore, to accurately recognize the position of an obstacle, it is important to detect the direction of the reflected point. In this work we use a method to obtain the direction by calculating it from the distance difference between two parallel ultrasonic transducers hence the phase-shift between the two signals.

One of the earliest systems, with two ultrasonic sensors [24], was only able to differentiate between walls and edges, using TOF and amplitude as source information. Afterwards, a new system with three active (movable) sensors [25], providing TOF and amplitude information, was able to classify the reflectors as *small* (edges) or *large* (walls and corners).

Later on, a special combination of two transmitters and two receivers [26] using only TOF information had the ability to detect and distinguish among the three

15

basic reflectors. A triaural system which has the ability to determine the curvature of any reflector between the edge and the wall is reported in [27]. The three basic reflectors, planes, corners and edges, can also be identified by a four-TOF sensor system [28].

Lastly, a simple system with only two rotative Polaroid transducers and TOF information [29] was able to detect and distinguish all the basic reflectors. The ME-EERUF (Multi-echo Error Eliminating Rapid Ultrasonic Firing) system [30] with only two transducers and TOF processing together with an active firing scheme shows ability to detect and classify on real time standard reflectors as edges, corners and walls. ME-EERUF allows high data acquisition rates with a high level of error rejection, it is easy to implement with simple sensor configurations, providing essential information for reflector recognition.

The perception of reflector position and classification is of great importance, allowing the implementation of new methods for real-time map building, and can be an important source of information for robot localization, obstacle avoidance, safe navigation and environment representation [31, 32, 33]. Therefore in search for a solution researchers and engineers have developed a variety of sensors, systems and techniques for mobile robot relative and absolute positioning [34, 35, 36, 37]. In absolute positioning both lateral (x,y) and angular (θ) positions are measured relative to predefined objects. Relative positioning on the other hand, the position of a mobile system is determined relative to the previous position. We show in this work that the position of a planar indoor obstacle can be defined by its lateral and angular position and applied in obstacle detection and avoidance.

2.2 Sonar compared to Infrared range finders

Recent advances in sensing technology have made available optical rangefinders that do in fact approximate a ray-trace scanner. Devices that operate on a phase

measurement principle are the best. The first phase-based rangefinder was developed by AT&T Bell Laboratories in the mid-1980s [38, 39]. The AT&T rangefinder can take a complete, dense scan in less than one second. Bell labs do not produce a commercial version, but have licensed the technology to other companies. At the Oxford robotics group, Brownlow, Adams, and Tarassenko have recently developed a novel phase-based ranging device that may out-perform the AT&T sensor [40], since it is capable of resolving phase shifts in the received light signal of the order 0.1^0 over a 50 dB dynamic range. Optical rangefinders vary in scale from laser-based systems, of the type used by Hinkel *et al.* [41], to inexpensive amplitude-based infrared devices, as used by Flynn [42] and Connell [43]. The former offers precision at high cost, while the latter cannot provide accurate range information because of their sensitivity to surface reflectance properties. The AT&T design achieves comparable performance to laser-based systems at much lower cost.

The transmitted signal from an infrared range finder is modulated at 5 MHz, enabling direct range information to be obtained by measuring the phase shift between transmitted and received waveforms. An automatic gain control amplifier overcomes variations in signal strength due to attenuation losses and changing surface reflectance properties. A useful operating range of twenty feet is obtained, with a typical range resolution of one inch. Because an infrared Light Emitting Diode (LED) is used instead of a laser, potential eye safety problems are avoided. Cox [39] has presented the successful use of the device to achieve on-the-fly localization with a priori map. The AT&T rangefinder can take a complete, dense scan in less than one second. Given this fact, sonar seems unreliable and inaccurate. However, we believe that sonar's great potential lies in the fact that typical indoor environments contain surprisingly few acoustic targets. The task of achieving and maintaining correspondence between observations and map targets will be considerably easier in many environments with acoustic sensing. Interpretation paradigms are possible in which single, isolated returns can be used

to update directly the vehicle position. The limitations imposed by physics must be distinguished from the limitations of the Polaroid ranging system design criteria. Sonar's rate of data acquisition is limited by the speed of sound, which is 343.2 meters per second at 20 degrees Celsius. Through a policy of directed sensing, it should be possible to obtain and process 100 returns per second in tracking a target one meter away. Very high vehicle position update rates should be possible if directed sensing strategies are combined with a faster firing capability. To prevent interference among sensors, the firing of multiple sensors must be coordinated, but careful engineering should be able to meet this requirement. Frequency modulation and amplitude-based interpretation present the opportunity for higher resolution [44]. However, the simple TOF system has not been pushed to its resolution limit. Carefully engineered hardware could completely eliminate the effects of weak returns and assure constant target visibility over all ranges. We believe sonar is a much better sensor for position estimation than its reputation would suggest.

The straightforward use of a ring of transducers to form a "sonar bumper" is fraught with difficulty, though Borenstein [31] success shows it can be done. Their use of very rapid sensor firing rates agrees with the concept of continuous map contact. Dynamic operation will require interpretation strategies that can accommodate fast sensor update rates. Kuc [47] is the only researcher who has made the claim of 100 percent reliable collision prevention, using a good model of edge visibility and conservative path planning

2.3 Sonar compared to vision

Vision is by far our most powerful sense. However, consider a typical Charge Coupled Device (CCD) camera as a sensor that has a wealth of information of the world around the system at an instant. All that is needed is the actual position of the obstacle defined by the co-ordinates x, y, and Φ. In an environment with a large number of obstacles [45], it is impossible to predict, or usefully process the

18

wealth of information given as sensor data in the form of hundreds of thousands of eight bit numbers every 40 milliseconds in approximation. This is because the information is embedded in a huge array which is impossible to extract at an instant.

A sonar system uses, on average, three 12-bit numbers to update the robot's position each time it moves. It is therefore easier to implement a sonar sensor on a robot system as an accurate and reliable obstacle detection system.

CHAPTER THREE

THEORY

3.1 Angle measurement of obstacles by phase-shift method

3.1.1 The principle of measurement of the obstacle angle

In an indoor environment, flat obstacles have specular characteristics, therefore, the real reflected point is not located on the transducer's line of sight. This is because an echo from the normal incidence only, returns to the transducer, since ultrasonic directivity is not so sharp in air. To accurately recognize the position of an object, it is important to recognize the direction of the reflected point. One method that can be used to obtain the direction is to calculate it from the distance difference between two parallel receivers.

In a conventional ultrasonic sensor for a mobile robot, the range value is obtained by pulse-echo method, and the direction of the reflected point is assumed to be the line-of-sight of the transducer. However, in reality, the echo observed by the receiver is limited to the reflection from the foot of the perpendicular line of the obstacle that is drawn from the transducer; this is because of the width of the ultrasonic beam and mirror like characteristics of the obstacle's surface. Therefore, a conventional ultrasonic sensor does not provide the reflecting point accurately, and it is inconvenient to use such a system with a robot to recognize obstacles. One way to overcome this problem of conventional ultrasonic ranging is to not only measure range values, but also the direction of the reflecting point. By such a measuring system, the inclination angle of the obstacle to the line-of-sight of the transducer is detected based on the feature that an ultrasonic wave reflects specularly on the surface of the obstacle. Hence, when a robot located at the origin of a set of polar coordinates finds a reflected point (r, θ), as shown in the figure 3.0, an obstacle of inclination angle θ is expected to exist. In a conventional ultrasonic ranging system, when a robot needs to recognize the

inclination angle of an obstacle, it must obtain two range values at different positions, this is not a real-time process. However, when the inclination angle of obstacles is detected, a robot is able to revise its relative position and the orientation of obstacles in real-time. By considering a system consisting of one transmitter and a pair of receivers as shown in the figure 3.0, the direction of the reflecting point is the relation between θ and the difference dl of the path length of travel of the detected echo by the two receivers given by

$$\sin \theta = \frac{dl}{d} \tag{4}$$

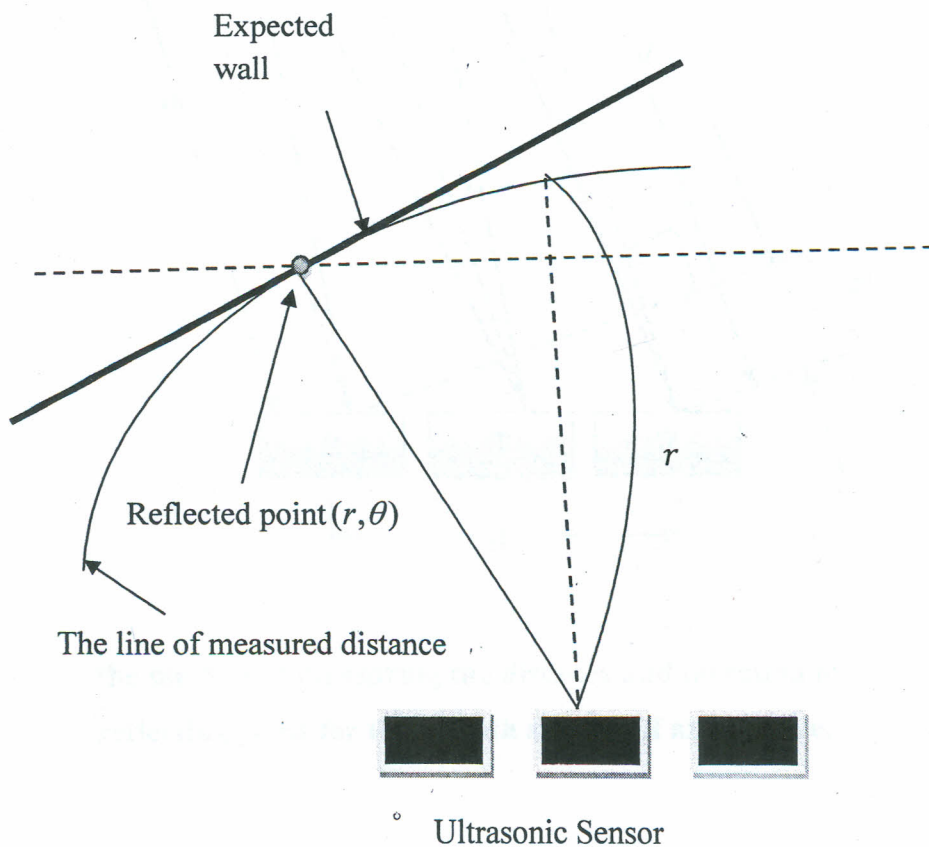where d is the distance between the two receivers as shown in figure 3.1.

Expected
wall

Reflected point (r, θ)

r

The line of measured distance

Ultrasonic Sensor

Figure 3.0   **The expected obstacle from measured distance r and direction θ**

21

dl is obtained by
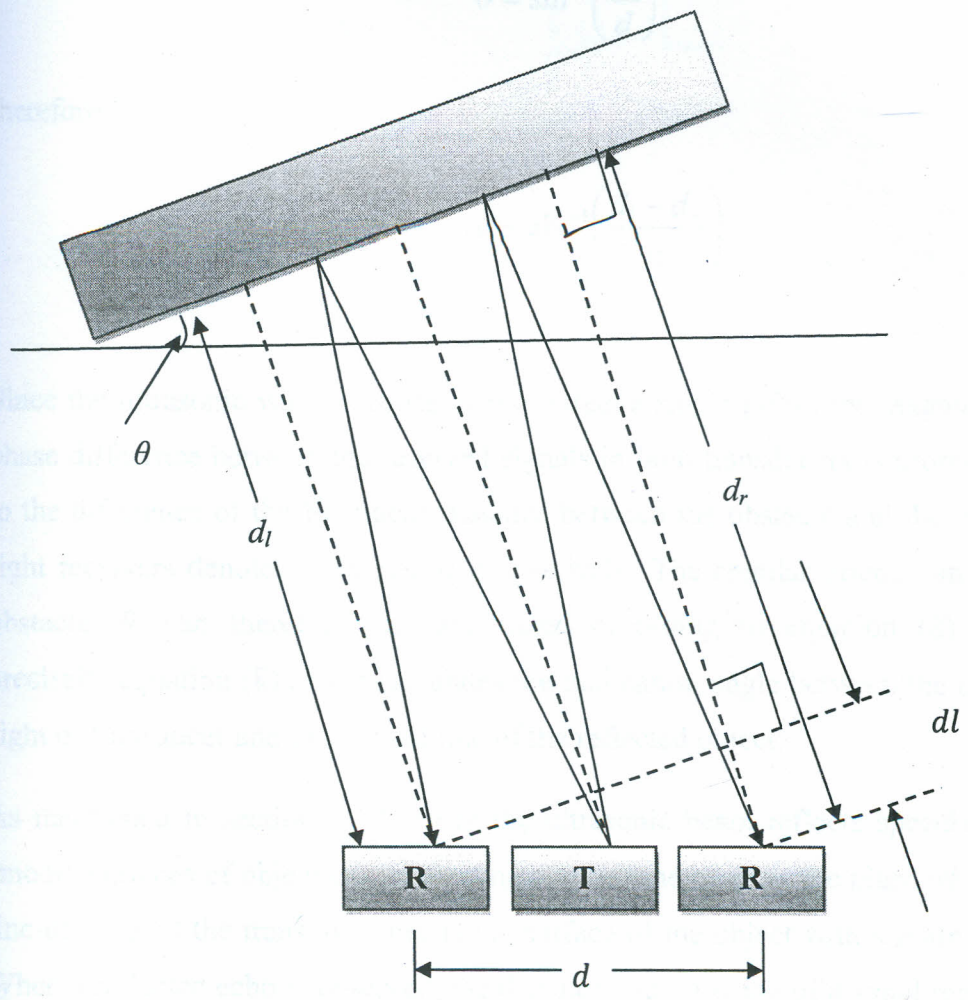
$$dl = (t_l - t_r)v \qquad (5)$$

Figure 3.1   the method of measuring the distance and direction of reflecting point for the smooth surface of an obstacle.

therefore

$$dl = (d_l - d_r) \qquad (6)$$

where v is the speed of sound in air, t_l and t_r are the TOFs which are measured on the left and the right receivers respectively. The angle θ can be approximated by equation (7)

$$\theta = \sin^{-1}\left(\frac{dl}{d}\right) \tag{7}$$

therefore

$$\theta = \sin^{-1}\left(\frac{d_l - d_r}{d}\right) \tag{8}$$

Since the ultrasonic wave consists of more than a single pulse, the magnitude of phase difference between the received signals in both transducers is proportional to the difference of the Euclidean distance between the obstacle and the left and right receivers denoted by d_l and d_r respectively. The angular orientation of the obstacle, θ, can therefore, be determined according to equation (8). More precisely, equation (8) above calculates the inclination angle between the line-of-sight of transducer and the normal line of the reflected object.

As mentioned in section 3.1.1, since the ultrasonic beam reflects specularly on smooth surfaces of objects, the reflecting point of the beam is the place where the line-of-sight of the transducer meets the surface of the object with a normal line. When a reflected echo is observed, the distance and direction of a small region on the surface of the object are measured. A small region on the surface with a normal vector will be referred to as a surface element of the obstacle as shown in figure 3.2.
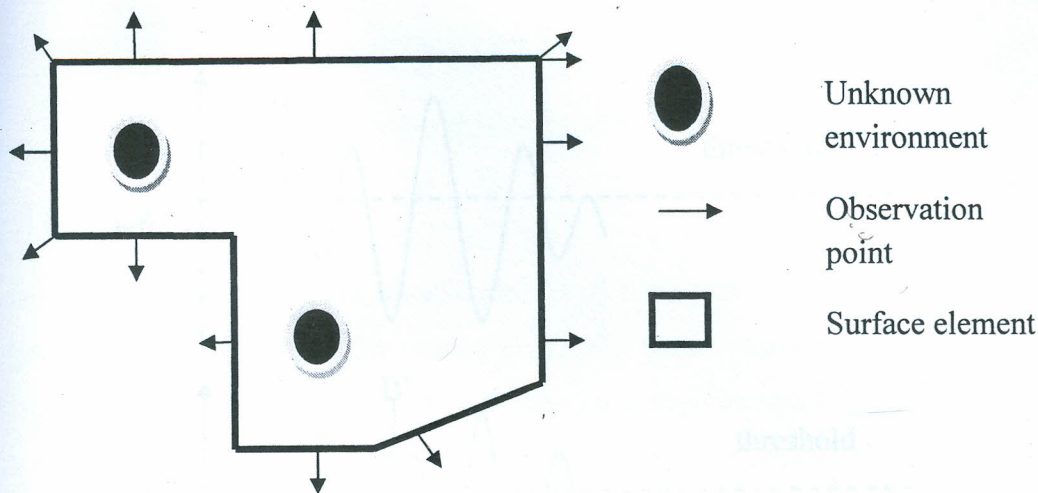
23

Figure 3.2   Example of surface element distribution

3.1.2 Errors in the direction measurement

The proposed system is able to measure angles using the difference between the left and the right range values. So, a shorter distance between the left and the right receivers may cause an error in the inclination angle. This is because of measuring the difference of TOF between the left and the right receivers. Usual TOF systems measure the time values when the amplitude of the echo waveform first exceeds a threshold level. So, a small difference in amplitude of the left and the right receivers may make a small difference to the TOF, and will lead to discrete angle errors as shown on figure 3.3.

For example, for both receivers, when the echoes first exceed the threshold level, they must be in the same phase, but if the m-th phase of an echo first exceeds the threshold level at left receiver and the n-th phase exceeds the threshold level at the right receiver, the angle error $d\theta$ is given by
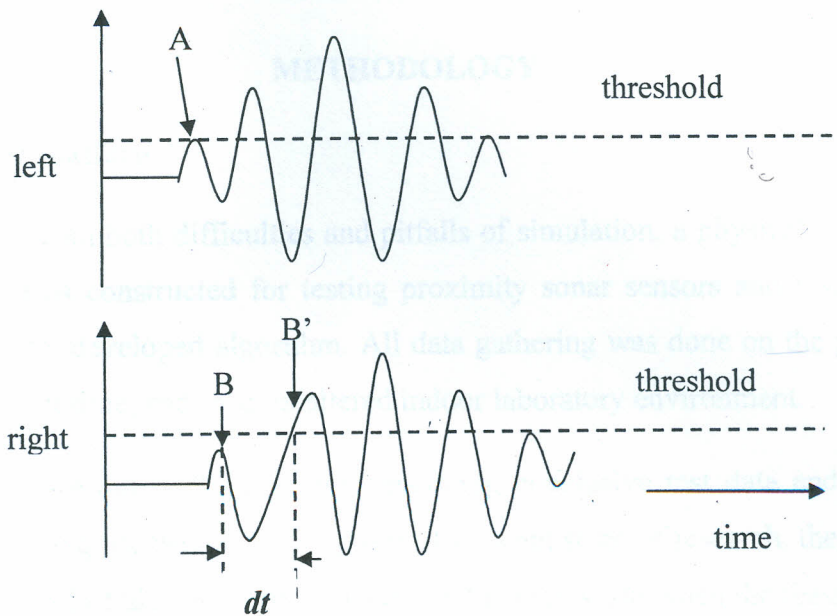
$$d\theta = \frac{\lambda}{2d}(m-n) \qquad (9)$$

Figure 3.3 The cause of error in discrete angle. To measure the inclination angle correctly, the same phases (both A and B) should exceed a threshold level. But in this case, in the left receiver, phase A exceeds the threshold level, but in the right receiver, phase B doesn't exceed but the phase B' does, so the T.O.F measurement has an error of about one period dt. This can cause a serious error in measurement of the angle.

where λ is an ultrasonic wavelength. That is, the system sometimes has a discrete angle error whose step size is $\frac{\lambda}{2d}$. This error in the reflecting direction relating to the ultrasonic wavelength is a similar phenomena to the grating lobe of the beam width of the detector. To eliminate such an error, the condition ($m = n$) is necessary, but generally it is difficult to keep such a condition. The mechanism used to find this kind of error is, to take multiple readings at the same point and process them with grating-lobe elimination algorithm after getting the statistical distribution of the calculated direction. [34]

CHAPTER FOUR

METHODOLOGY

4.1 The test platform

In order to avoid both difficulties and pitfalls of simulation, a physical robot, the Polyrobot, was constructed for testing proximity sonar sensors and testing and debugging the developed algorithm. All data gathering was done on the physical system, in real time, and in an unaltered indoor laboratory environment.

Simulations are not well suited for generating conclusive test data and results. While they are quite useful for the proof-of-concept stage of research, they do not suffice as proof of algorithm functionality in the real world when the feasibility of the algorithms needs to be tested. A simulation generating successful data tells us much less than a simulation that fails. If an algorithm fails in simulation it will certainly not work in real world, but the converse is not necessarily true. A trustworthy simulation requires accurate modeling of the physical process involved. For mobile robots this means accurate modeling of the robot itself as well as its environment.

Modeling physical sensors has proven to be a difficult task. Kuc *et al* [46, 47] and Letovsky [48] provide analytical methods for modeling and interpreting sonar data, with varying degrees of complexity. In general, the more the physical sound of the sonar characterization, the more complex and computationally intensive it is to simulate. Not only do the simulations not run in real-time, but their failure to do so is due to reasons unrelated to the algorithm they are testing, for example, very often the speed of the simulation is limited by a variety of extensive modeling computation required in computational geometry and many other related reasons. Since writing a realistic simulator is a difficult task, many compromises are made to simplify it. Unfortunately, each such compromise acts to decrease the value of the simulation. For instance, many simulations use a

simple Gaussian to characterize sensory error and noise. This generates a sensor behavior often entirely different from that which will be observed in the real world.
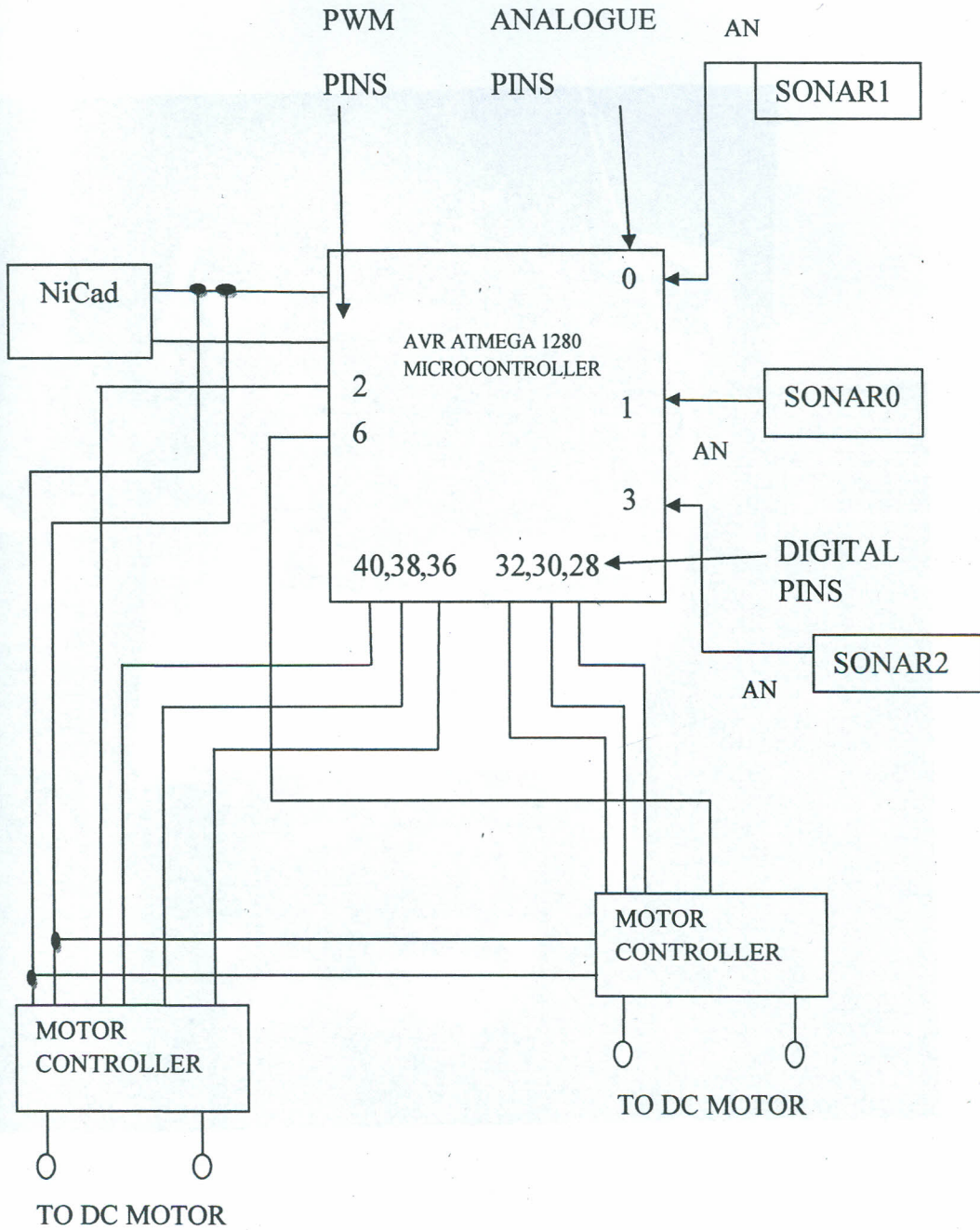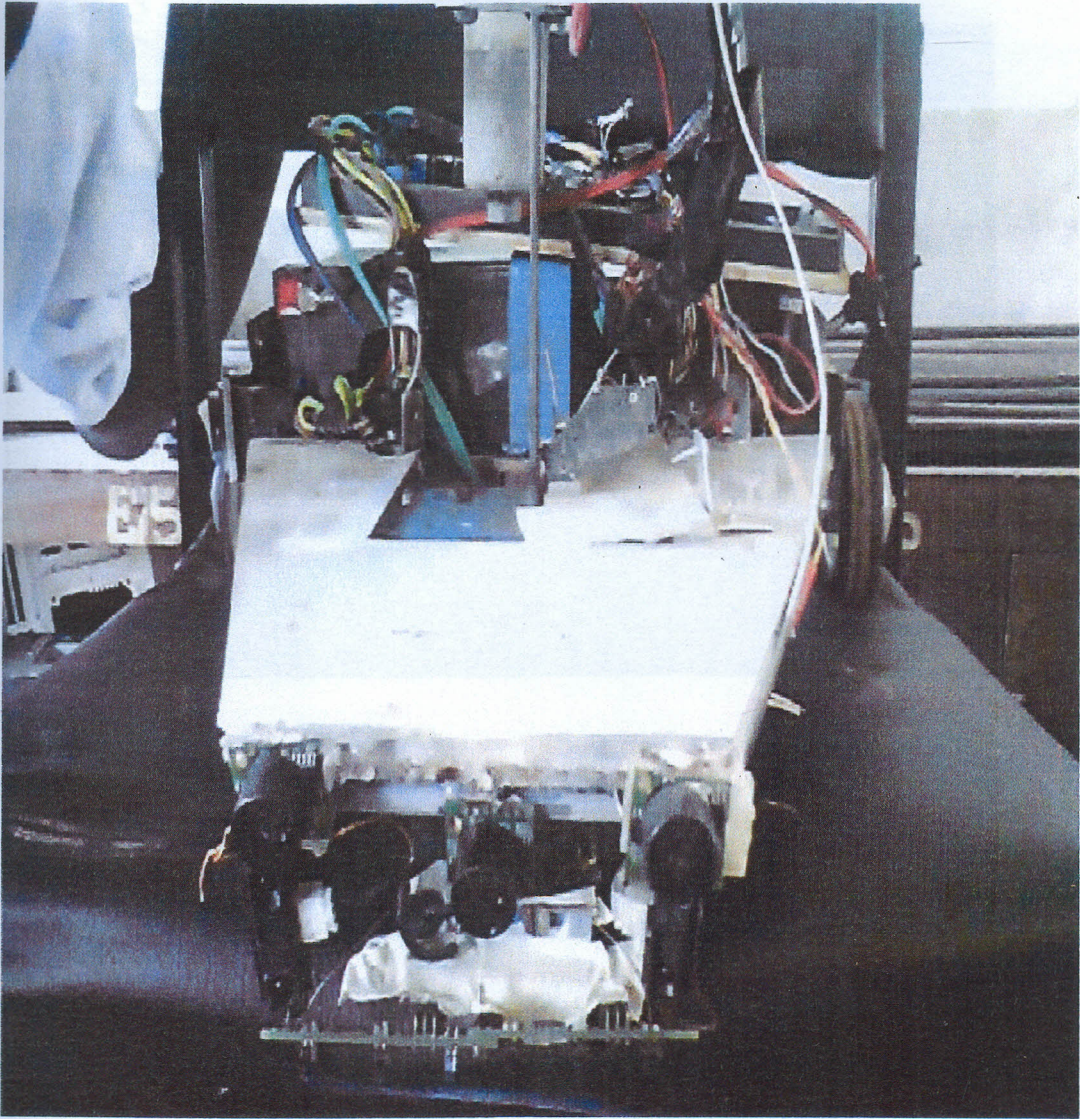
4.2 The Polyrobot

Figure 4.0 Schematic block circuit diagram of the Polyrobot

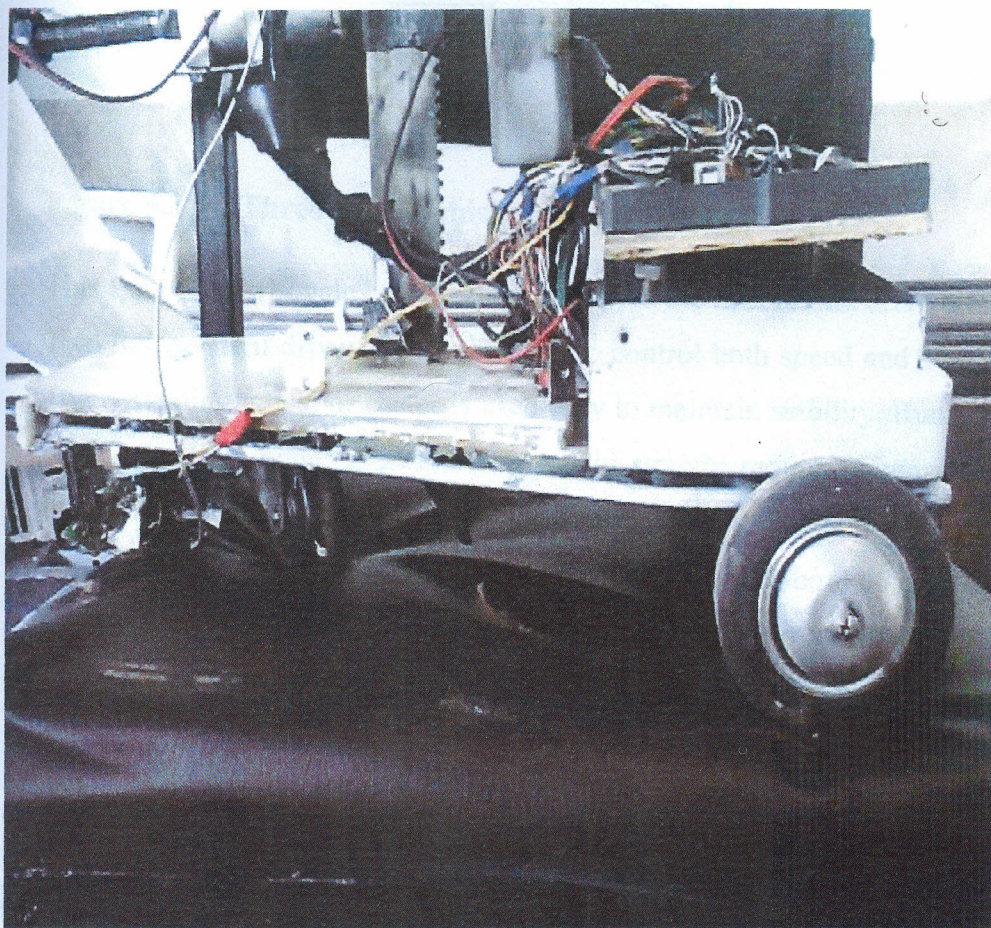**Figure 4.1   Front panel of the Polyrobot**

Figure 4.2   Sideview of the Polyrobot

4.2.1 Actuator design

The Polyrobot's only actuator is a Real World Interface three-wheeled circular robot base 5cm in diameter. The wheels and the top platform of the base are connected. This "tri-cycle" arrangement requires that the two drive wheels rotate at different speeds while the vehicle is turning. If the drive wheels are statically coupled to rotate at the same speed, "scrubbing" will occur. "Scrubbing" is the dragging or slippage of a wheel caused by a difference in required and actual speed. "Scrubbing" leads to excessive tire wear and odometry errors.
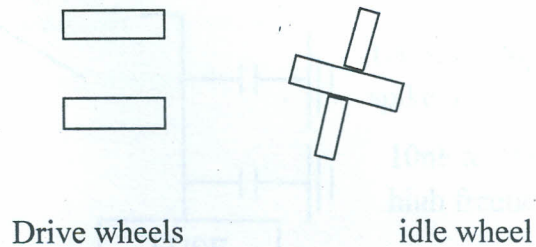
Drive wheels   idle wheel

Figure 4.3   Three wheel vehicle configuration

This type of a "tri-cycle" arrangement is called the differential drive arrangement. Two independent drive wheels are used to control both speed and steering angle. The remaining wheel or caster is used only to maintain stability. Running the two drive wheels at equal speeds will result in straight motion. Changes in vehicle direction are achieved by operating the drive wheels at different speeds. Equal but opposite wheel velocities will cause the vehicle to rotate about the mid-point of its drive wheels, thus producing the possibility of a Zero Turn Radius (ZTR) vehicle. The extreme maneuverability of ZTR vehicles has made this arrangement popular among researchers. Precise motor control and feedback are necessary to accurately control ZTR vehicles. Mechanical factors such as wheel slip, misalignment, and unequal tire diameter can also complicate trajectory tracking.

Since the robot can turn in place by an arbitrary angle, it can continuously follow any trajectory with discontinuous velocity. The built-in microcontroller board accepts rotational, velocity and acceleration commands

4.2.2 Controls

All the robots motions used in this study are provided by two motors: One for each of the two wheels (car drive). To control the motors, a 14A dual H-Bridge is used. The H-Bridge is the link between digital circuitry and mechanical action. The computer sends out binary commands, and high powered actuators rotate. Most often H-bridges are used to control rotational direction of DC motors.

30
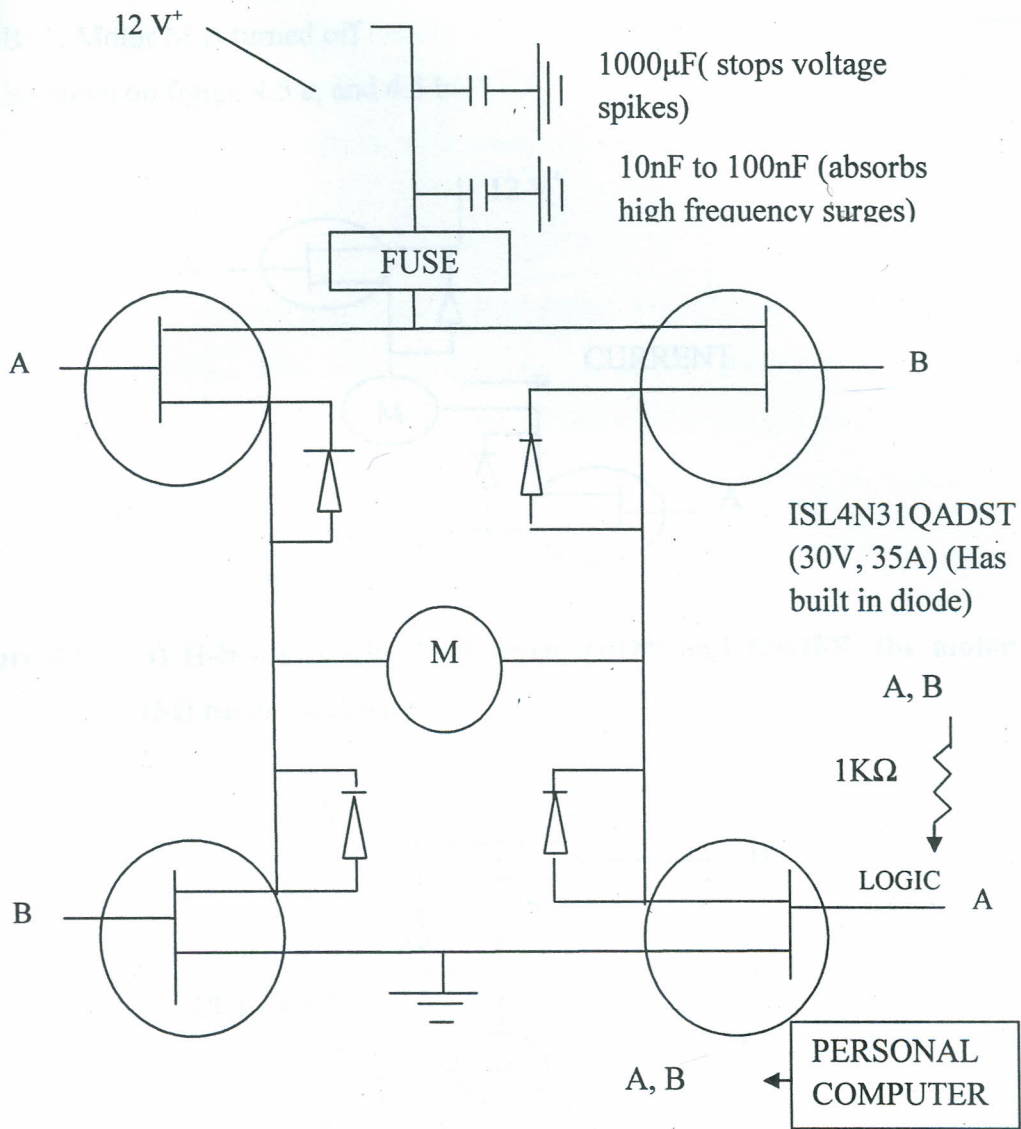
Figure 4.4   H- Bridge circuit with supporting circuitry

The top two are P-channel MOSFETs and the bottom two are N-channel MOSFETs which are connected to ground. In the above schematic the letters A and B are two control lines on which logic voltage is applied. Since there are two pins, and only a binary control, there are four possible outcomes.

A=0 B=0: Nothing happens, the motor M is turned off.

A=1 B=0: Motor rotates clockwise

A=0 B=1: Motor rotates counterclockwise

A=1 B=1: Motor M is turned off

This is shown on figure 4.5 a, and 4.5 b.

12 V⁺

A

CURRENT

M

A
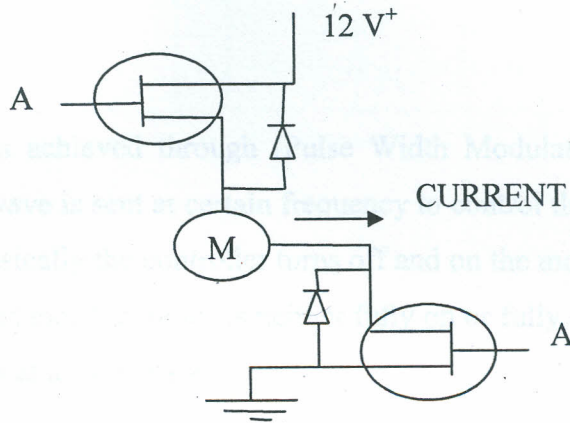
Figure 4.5 **a) H-bridge logic chart when A=ON and B=OFF: the motor (M) turns clockwise**

12V⁺

B

CURRENT

M

B

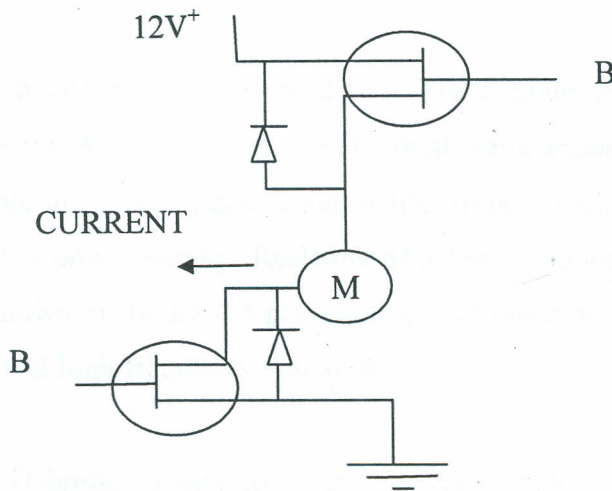**Figure 4.5** **b) H-bridge logic chart when A=OFF and B=ON: the motor (M) turns counterclockwise**

To operate a MOSFET, a voltage is applied to the gate (from the microcontroller), and suddenly a current of electrons passes through the other two pins. Basically the gate is attached to the digital output of the microcontroller and when the

digital output is turned on, 5V will be applied to the gate, turning the MOSFET on. The gate voltage controls the MOSFET internal resistance. Zero voltage makes the resistance too high for it to work while a high voltage has a very low resistance.

Speed control is achieved through (Pulse Width Modulation) PWM. PWM is when a square wave is sent at certain frequency to control the MOSFET as shown in figure 4.6. Basically the controller turns off and on the motor at very high rates. So through inductance the motor is neither fully on or fully off, but somewhere in between, such as at a slower speed.

Under PWM the motor torque remains the same whether fully on or only a percentage on. However, varying voltage for speed control reduces torque. So, with PWM maximum torque is achieved even for low speeds.

The MOSFETs have inbuilt protection diodes. These diodes prevent back currents from the DC motor. Across the motor leads, small value capacitors are attached to reduce electronic noise and increase motor life. In addition, a slow blow fuse is attached after the power supply. Resistors of a few ohms on the logic gate and capacitors as shown on figure 4.4 prevent the electronics components from large voltage surges and high frequency emission.

In summary, a H-bridge is used to control the robot motors. Pulses generated by the microcontroller helps dictate the speed and direction of each motor. These pulses are output signal generated by the microcontroller. The controller card controls each of the two motors independently and simultaneously by sending analog signals to the amplifiers. The motors run at speeds proportional to the PWM voltages.

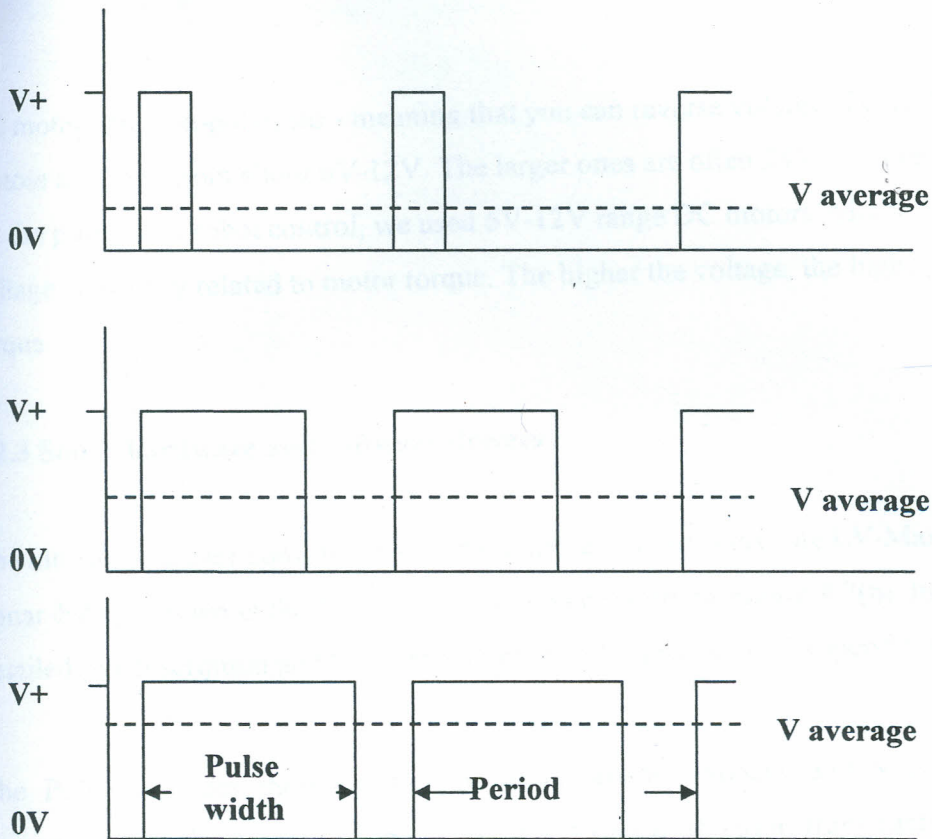**Figure 4.6** **Square waves at certain frequencies to control the MOSFETS**

The signals from the sensors are fed back to the controller card to calculate the direction and speed of the motor.

The selection of the motors had to meet the following requirements which were specified by the chassis (Drive Wheels):

- Drive motor requirements (at load)
- Maximum Continuous Torque
- Intermittent Peak Torque
- Speed
- Direction

34

DC motors are non-polarized - meaning that you can reverse voltage. Typical DC motors are rated from about 6V-12V. The larger ones are often 24V or more. But for the purpose of robot control, we used 6V-12V range DC motors. Motor voltage is directly related to motor torque. The higher the voltage, the higher the torque.

4.2.3 Sonar hardware and software drivers

The ultrasonic sensor considered and implemented in our study, the LV-Max Sonar-EZ1 is shown in the Figure 4.7(a) and its circuitry in Figure 4.7(b). Its detailed pin description and beam characteristics are provided in Appendix L.

The Polyrobot uses three of the ultrasonic sensors. Sonar1 and Sonar2 are mounted at the front panel of the robot at a distance of 10 cm from each other. Sonar0 is mounted directly below the two at a distance of 2cm and 5cm from one end. The former are used to obtain range data for angular orientation computation and the latter the range information is used to provide the exact execution point.

a)   b)

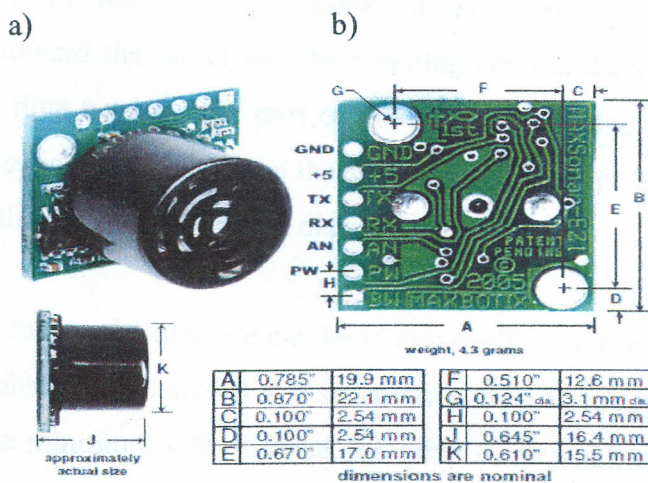| A | 0.785" | 19.9 mm | F | 0.510" | 12.6 mm |
B	0.870"	22.1 mm	G	0.124" dia.	3.1 mm dia.
C	0.100"	2.54 mm	H	0.100"	2.54 mm
D	0.100"	2.54 mm	J	0.645"	16.4 mm
E	0.670"	17.0 mm	K	0.610"	15.5 mm

weight, 4.3 grams

dimensions are nominal

Figure 4.7a, b. a) The LV-Max Sonar EZ1 sensor b) on board circuitry [49]

The sonar sensing devices, at a separation distance of 10 cm apart, are mounted on the front panel of the robot at a height of 8cm. At this height the sensors could not detect the ground as an obstacle. The devices are configured as shown in the Figure 4.8.
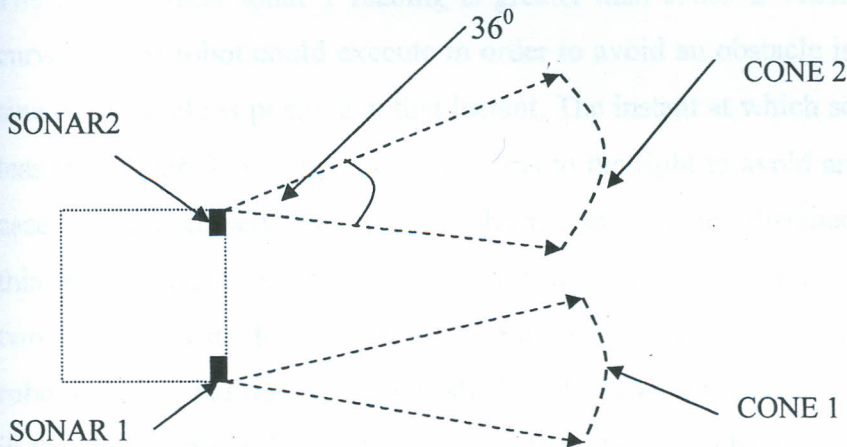

Figure 4.8   Robot with stationary sonar

Each sonar sensor detects obstacles in a 36 degree cone. The sensor has a maximum range of 2.43m to 3.05m but the area of interest is restricted to 0.30m radius so as to eliminate noise due to obstacles that are out of the robot's path. In the operation of the system, a pulse of electronically generated sound is transmitted toward the target and the resulting echo is detected by the receiver. The elapsed time between the start of the transmitted pulse and the reception of the echo pulse is measured. Since the speed of sound in air is known, the system can convert the elapsed time into a distance measurement.

As the robot moves the obstacle can be in any position within the two cones. The moment an obstacle is detected at a set distance of 0.30 metres radius, which we defined as the minimum safe distance, the robot starts making decisions based on range readings from sonar 1 and sonar 2. Using these readings logic functions developed are used to steer the robot away from obstacles.

From equation (8) and figure (3.1) we define sonar 1 readings as d_l and sonar 2 readings as d_r. Since we set the obstacle width as a constant the logic approach was restricted to range readings of sonar 1 and sonar 2, after sonar 0 (the middle sonar) records the minimum safe distance reading.

The instant when sonar 1 reading is greater than sonar 2 reading, the smallest curvature the robot could execute in order to avoid an obstacle is to the left. The sine of the angle is positive at that instant. The instant at which sonar 1 reading is less than sonar 2 reading, the robot turns to the right to avoid an obstacle. In the case where both sensors detect an obstacle at an equal distance simultaneously this indicates that the obstacle is an endless long obstacle for example a wall or two separate obstacles parallel to the transverse axis of the robot. In this case the robot reverses and makes a turn to the left. The above logic functions are executed in the avoid loop of the navigation algorithm shown in chapter 5. The algorithm is uploaded in the application flash memory of the AVR ATMEGA1280 microprocessor. An AVR ATMEGA1280 microprocessor is used for processing the distance calculations. The distance value is returned through a RS232 port to the control computer. The system is powered by an isolated power supply of 5V DC at 0.5 amps.

Taking the data input from an obstacle detecting sensor comes in a variety of formats depending on the onboard circuitry. Precise and accurate sensors like the LV Max Sonar EZ1 are often extremely sensitive and a byproduct of sensitivity is always a fluctuation of output values. This was taken care of by averaging sonar signatures at instances when $d_l = d_r$, $d_l < d_r$ and $d_l > d_r$ all at an instant when the robot is at 30 cm from the obstacle taken within a given period of time. The averaging was done for each sensor since they have different sensitivities. The sonar signatures are tabulated in table 5.0, table 5.1 and table 5.2 in chapter 5. The LV-Max Sonar-EZ1 has a buffer that holds the previous output until a new output

is available, thus the determining factor of how to often store values is the reaction time of the robot to avoid obstacles.

4.2.4 The power supply

The power sources chosen for the Polyrobot's operations are a 12V battery, regular and high capacity NiCads. The motors are running off three 1.2V 4000mAh NiCads for a total of 3.6V (Vmotor). The motor controller uses a 12V battery (Vmosfet) to properly bias the MOSFETs driving the motors. The AVR ATMEGA1280 microprocessor and its related electronics have its own 5V regulator. V_{CC} is electrically isolated to Vmosfet and Vmotor which shares a common ground (earthed).

NiCads are good for small to medium size range robots like the Polyrobot. This is because they have a high current output and can be recharged within one or two hours. However, constant recharging leads to memory effect, such that once recharged the charge stored does not last for long. To minimize this effect, before recharge it is advisable to fully discharge the NiCad.

4.2.5 The CPU

The microcontroller chosen for this robot is the AVR microcontroller. There are many variations of this microcontroller and some, especially models with large internal EEPROM are very difficult to obtain. There are many AVR based microcontroller available commercially. We decided to use AVR ATMEGA1280 for its technical specification. Here is a short technical specification summary of AVR ATMEGA1280 microprocessor:

- 53-pin ATMEGA microprocessor
- 32K of battery backup static RAM
- 12 PWM motor ports (output)

38

- 16 analog ports (input)
- 10 Communication ports
- 5V and 3.3 V supply

The AVR core combines a rich instruction set with 32 general purpose working registers. All the 32 registers are directly connected to the ALU, allowing two independent registers to be accessed in one single instruction executed in one clock cycle. The resulting architecture is more code efficient while achieving throughputs up to ten times faster than conventional CISC microcontrollers.

The ATmega1280 provides the following features: 128K bytes of In-System programmable flash with read-while-write capabilities, 4K bytes EEPROM, 4K bytes SRAM, 53 general purpose I/O lines, 32 general purpose working registers, RTC, four flexible timer/counters with compare modes and PWM, 2 USARTs, a byte oriented two-wire serial interface, an 8-channel, 10-bit ADC with optional interface, also used for accessing the on-chip debug system and programming and six software selectable power saving modes. The idle mode stops the CPU while allowing the SRAM, timer/counters, SPI port, and interrupt system to continue functioning. The power-down mode saves the register contents but freezes the oscillator, disabling all other chip functions until the next interrupt or hardware reset. In power-save mode, the asynchronous timer continues to run, allowing the user to maintain a timer base while the rest of the device is sleeping.

The ADC noise reduction mode stops the CPU and all Input/ Output modules except asynchronous timer and ADC, to minimize switching noise during ADC conversions. In standby mode, the crystal/resonator oscillator is running while the rest of the device is sleeping.
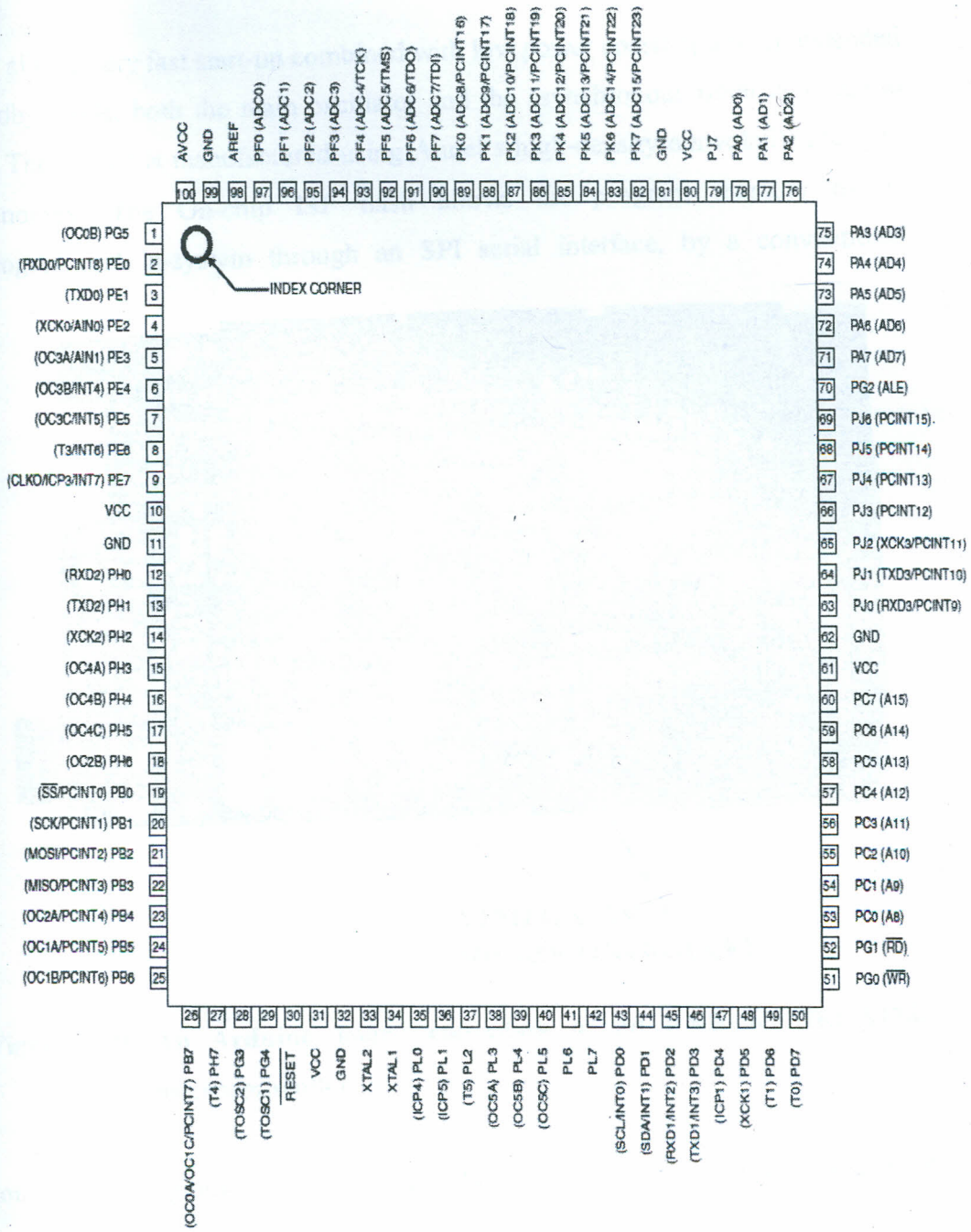
Figure 4.9   Pin configuration of an AVR ATMEGA1280 microcontroller

This allows very fast start-up combined with low power consumption. In extended standby mode, both the main oscillator and the asynchronous timer continue to run. The device is manufactured using Atmel's high-density nonvolatile memory technology. The On-chip ISP flash allows the program memory to be reprogrammed in-system through an SPI serial interface, by a conventional
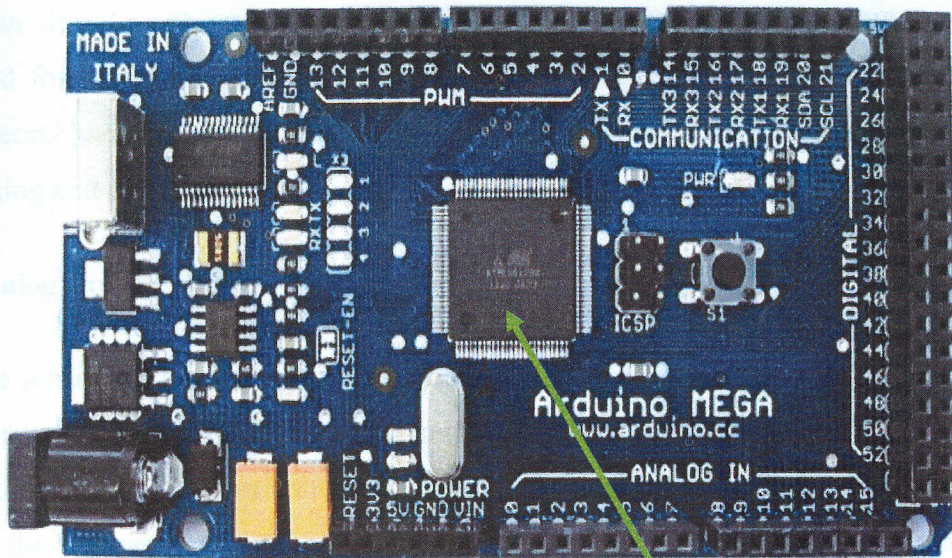
ATMEGA 1280
MICROCONTROLLER

Figure 4.10   An   Arduino   board   consisting   of   an   AVR   ATMEGA1280   microcontroller

nonvolatile programmer or by an On-chip boot program running on the AVR core.

The boot program can use any interface to download the application program in the application flash memory. Software in the boot flash section will continue to run while the application flash section is updated, providing true read-while-write operation. By combining an 8-bit RISC CPU with in-system self-programmable flash on a monolithic chip, the ATmega1280 is a powerful microcontroller that

41

provides a highly flexible and cost effective solution to many embedded control applications. The ATmega1280 is supported with a full suite of program and system development tools including: C compilers, macro assemblers, program debugger/ simulators, in-circuit emulators, and evaluation kits. Its detailed pin description is provided in appendix M [50].

4.2.5.1 Input/output ports

Input/output ports are an important feature on a microcontroller. Input ports are used for taking in sensor data, while output is used for sending commands to external hardware such as DC motors. There are two types of Inputs/Output ports; analog and digital.

Analog Input Ports

The sensors of the Polyrobot are connected to the analog input ports. Also known as an ADC, they receive analog signals and convert them to a digital number within a certain numerical range. Analog is a continuous voltage range provided by the sensor system that converts range information to voltage values, in this case, between 0 volts (LOW) and 5 volts (HIGH). However since computers can only operate in the digital realm with 0's and 1's the microcontroller converts an analog signal to a digital signal. First, the analog is measured after a predefined period of time passes. At each time period, the voltage is recorded as a number. This number then defines a signal of 0's and 1's. The advantage of digital over analog is that digital is much better at eliminating background noise.

Since the ATMEGA1280 features a 10-bit successive approximation ADC, connected to an 8-channel analog multiplexer, it has a range of 1024 obtained numerically as shown in equation (10).

$$2^{10} = 1024 \qquad (10)$$

Therefore, if a sensor reads 0V to the eight bit ADC, this would give you a digital output of 0 and 5V would give a digital output of 1023.

Digital I/O Ports

Digital ports are like analog ports, but with only 1 bit hence a resolution of 2 – on and off obtained numerically as shown in equation (11).

$$2^1 = 2 \tag{11}$$

Since they are for signal output we used them to control the DC motors. Therefore a high 5V signal turns the motor on and a low 0V to turn it off. To turn the motors at a given speed, a square wave for PWM is sent as shown in figure 4.6. As explained in section 4.2.2, square waves controls the DC motor H-Bridges by turning them on and off at a fast rate.

4.3 The Programming Environment

The Polyrobot software was written in Arduino C version 11. The Arduino IDE (also known as integrated design environment or integrated debugging environment is a software application that provides comprehensive facilities to computer programmers for software development. It (consists of source code editor, a compiler and/ or interpreter, build automation tools and a debugger) is a cross-platform application written in Java which is derived from IDE made for the processing programming language and the wiring project. It includes a code editor with features such as syntax highlighting, brace matching and automatic indentation, and is capable of compiling and uploading programs to the board with a single click. There is typically no need to edit make files or run programs on the command line.

The Arduino IDE comes with a C library called "Wiring" (from the project of the same name) in which many common input/ output operations are much easier.

Arduino programs are written in C although users only need to define two functions in order to make a runnable program:

setup()- a function run once at the start of a program which can be used for initializing settings, and loop() - a function called repeatedly until the board is powered off.

Arduino programs can be divided in three main parts: structure, values (variables and constants), and functions. [51].

The Polyrobot's software is a collection of behaviors which receive inputs from the sonar sensors. Behaviors can output commands to actuators (wheels). Since the drive wheel is the only actuator on the robot, it is controlled by a dedicated low level behavior [52].

In order to avoid the pitfalls and difficulties in simulation, the algorithm was implemented and tested on a physical robot, the Polyrobot.

4.4 Navigation

4.4.1 Motivation

The motivation behind the presented approach was to implement an intuitive navigation method, in contrast to some analytical approaches taken to achieve a similar goal. The goal is to implement navigation as a result of a collection of interacting behaviors. Each behavior consists of a set of rules associating some conditions in the world with appropriate actions. The rules are designed to be intuitive, and are of the form: "if the orientation of the obstacle is such that $\theta>0$ turn left". A set of important states of the world is selected and defined as a set of sensory patterns. Each pattern triggers the appropriate reflex behavior. Since the world provide continual stimuli, some sets of reflexes are activated at all times, resulting in a continuous stream of actions. The combinations of these actions results in the desired emergent behaviors.

44

4.4.2 Navigation Rules

The goal of the navigation behavior is to detect obstacles in the world and avoid collision with both static and dynamic obstacles in a surrounding indoor environment. The avoiding behavior is simply a survival mechanism while obstacle detection is a basis of the robot's perception of the world. The navigation rules rely on two distinct regions around the robot. In order of increasing radii from the robot these are: the minimum safe distance (30cm) and the danger zone (15cm). See the figure 4.11.

These boundaries utilize the short distance accuracy of sensors to keep the robot neither too close nor too far from the objects in the world. The robot avoids any obstacles within the danger zone by starting to make decisions while at the minimum safe distance and avoiding getting too close to the obstacle.

The choice of these distances is empirical, based on the robot's velocity which is determined by the PMW voltages. The average speeds of the motors proportional to the PWM voltages allows the Polyrobot to prevent collision with all static and most dynamic obstacles within 30 cm; this defines the minimum safe distance. Any dynamic obstacle which unexpectedly appears within the danger zone, (a radius of 15 cm to obstacle) and moves towards the robot at a velocity nearly equal or higher than the robot's will cause a collision. An obstacle in the minimum safe distance or further can be avoided once detected. Within this distance the robot does not veer too far from the obstacle but still has some area within which it can move. However it should be noted that in the algorithm logic functions developed from sonar range values collected ensured that the algorithm does not keep the robot at a constant radius away from the obstacle, but within a desirable range. That range is defined around the minimum safe distance.

Minimum safe distance

Danger Zone
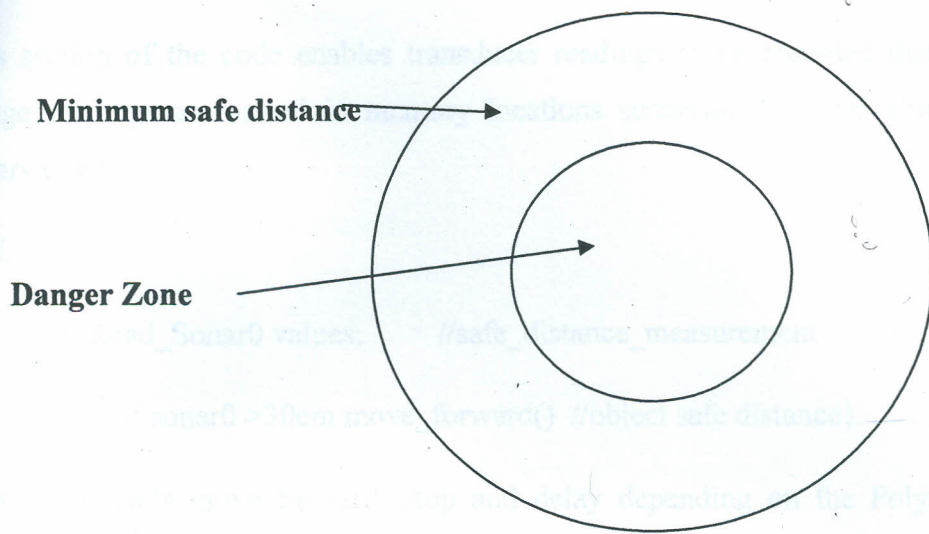
Figure 4.11 A schematic of the distance circles defining the two regions around a robot. These regions are used to implement navigation rules which combine to produce an effective obstacle avoidance behavior of the robot system.

These radii were learned by the robot, through trial and error. While optimized for the Polyrobot's parameters, they can easily be adapted to fit a robot with a different geometry or velocity constraints.

The desired object avoidance behavior is as a result of the following simple rules:

Ranging:

{read and record sonar_values in the assigned memory location (Sonarvalue0,Sonarvalue1,Sonarvalue2)

Sonarvalue0 = analogRead(Sonar0);

Sonarvalue1 = analogRead(Sonar1);

Sonarvalue2 = analogRead(Sonar2); }

This section of the code enables transducer readings to be recorded distinctly. Range readings are stored in memory locations sonarvalue0, sonarvalue1 and sonarvalue2.

Roll:

> { Read_Sonar0 values;   //safe_distance_measurement
>
>   if sonar0 >30cm move_forward() //object safe distance}

This code sends move forward, stop and delay depending on the Polyrobot's distance from the danger zone. It enables the robot to move safely forward.

If there is no obstacle in the minimum safe distance range recorded by the middle sonar (sonar0), the robot continuously moves forward. Rather than getting discrete instructions to move forward to a certain location, the robot constantly receives "encouragement" to keep moving forward a perpetually escaping goal, which results in smooth, continuous motion.

If the middle transducer (sonar0) detects an obstacle within the danger zone, the robot stops and delays momentarily (1000 ms). This is a defensive behavior which allows the robot to get out of tight spots and away from unexpected obstacles. Consequently, if an obstacle is moving (for example a person moving towards the robot) the robot will stop briefly. It then waits for the next sensory information. If the obstacle disappears based on sensor reading, it resumes motion in its original direction. If the obstacle is still detected, the robot makes the next decision, turning away.

Roll alone provides the robot with the basic safe straight-line motion. It allows it to move forward and stop and delay when necessary.

Avoid:

```
{ Read_Sonar0 values;

        Read_Sonar1 values;

        Read_ Sonar2 values;

    if (sonar0<= 30 cm {stop();} // start making decisions

    if ((Sonar1-Sonar2)>0 ) {turn left();}// object inclined at a positive
angle

    if((Sonar1-Sonar2)<0) {turn right();}// object inclined at a negative
angle

    if((Sonar1-Sonar2)=0) {reverse();}// object perpendicular to robot axis

}
```

If an obstacle is detected within the danger zone and the range reading of left transducer (sonar1) is greater than the range reading of the right transducer (sonar2) such that the angular orientation of the obstacle θ is positive, the robot turns to the left and if the range reading of the left transducer is less than that of the right transducer such that the angular orientation of the obstacle θ is negative, the robot turns to the right. The robot basically consults its side sonars to determine the safe direction in which it turns. It turns in a direction which is not occluded by close obstacles. In conjunction with roll these rules result in emergent collision-free behavior. The robot moves freely around obstacles and is only forced to reverse if an unexpected obstacle appears on its way. Any static obstacle is detected and avoided by veering either to the left or right. Reversing is a defense-mechanism, which is useful with dynamic obstacles, endless obstacles like a long wall and two separate obstacles parallel to the transverse axis of the robot but rarely gets activated in case of static obstacles. The resultant robot

behavior is shown in Figure 4.12 for a combined roll and avoid loops. The dark shades represent obstacles.

KEY

LABORATORY
BENCHES

STAR
S

END
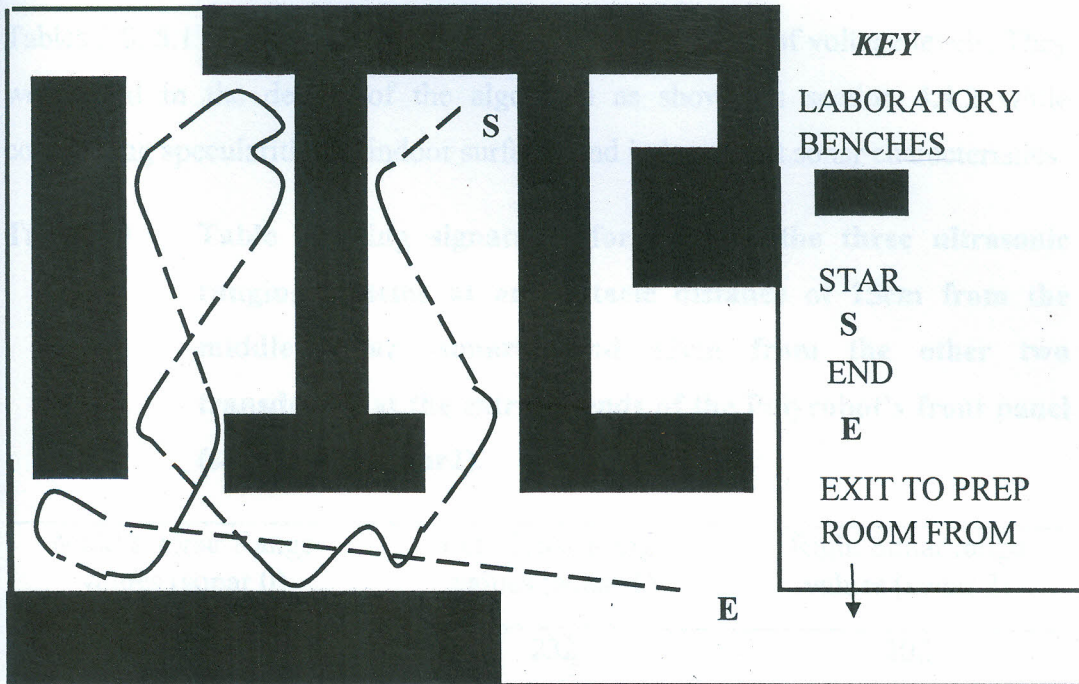E

EXIT TO PREP
ROOM FROM

Figure 4.12   **A combined roll and avoid behavior. Roll produces straight-lines path segments indicated by dotted lines. Path segments showing curves are generated by avoid and are highlighted by continuous lines.**

CHAPTER FIVE

RESULTS AND DISCUSSION

5.1 Sonar signatures

Tables 5.0, 5.1 and 5.2 present sonar range values in terms of voltage levels. They were used in the design of the algorithm as shown in section 4.4.2 while considering specularities of indoor surfaces and independent sonar characteristics.

Table 5.0   **Table showing signatures for each of the three ultrasonic ranging systems at an obstacle distance of 15cm from the middle sonar (sonar0) and 12cm from the other two transducers at the extreme ends of the Polyrobot's front panel (sonar1 and sonar2).**

Middle sonar Range values (sonar 0)	Left Sonar Range values (sonar 1)	Right Sonar range values (sonar 2)
424	232	202
422	235	207
445	232	200
437	235	205
429	232	207
418	236	202
422	233	207
424	236	207
423	235	205
422	233	207

Table 5.0 presents the signatures for each of the three ultrasonic ranging systems at an obstacle distance of 15 cm from the middle sonar (sonar0) and 12 cm from the other two transducers at the extreme ends of the Polyrobot's front panel (sonar1 and sonar2).

Table 5.1   **Table showing sonar signatures for two ultrasonic ranging systems at the extreme end of the front panel of the robot at an obstacle distance of 15cm from the left transducer (sonar 1) and 21cm from the right transducer (sonar 2).**

Left Sonar Range values (sonar 1)	Right Sonar range values (sonar 2)
160	373
152	368
160	372
160	376
162	372
160	375
165	368
156	372
164	372
167	368
162	375
162	372
162	371

Table 5.1 is a table of the signatures for two ultrasonic ranging systems at the extreme end of the front panel of the robot at an obstacle distance of 15cm from sonar 1 and 21cm from sonar 2.

Table 5.2   Table showing sonar signatures for two ultrasonic ranging systems at the extreme end of the front panel of the robot at an obstacle distance of 21cm from the left transducer (sonar 1) and 15cm from the right transducer (sonar 2).

Left sonar range values (sonar 1)	Right sonar range values (sonar 2)
263	166
269	165
266	160
260	169
263	163
269	166
260	164
264	164
261	162
262	160
263	165
265	160
263	164
261	164
263	160

Table 5.2 gives signatures for two ultrasonic ranging systems at the extreme end of the front panel of the robot at an obstacle distance of 21cm sonar 1 and 15cm from sonar 2.

5.2 Discussion of results

The data in tables 5.0, 5.1 and 5.2 are consistent for each sensor and the range values depend specifically on tolerance variations of the transducers during manufacturing and resolution of each sensor respectively since the target is common to all the three sensors.

Resolution is the minimum change in distance that can be measured by a sensor. The resolution of a range measurement made with an ultrasonic sensor is influenced by many factors, which include the accuracy of the time measuring circuits, ultrasonic frequency and the averaging capabilities of the sensor assuming no turbulence along the sound path. The AVR Atmega 1280 microcontroller contains a 10-bit analogue to digital converter. This means that it maps input voltages between 0 and 5 volts into integer values between 0 and 1023. This yields a resolution between readings of:

$$\frac{5V}{1024 \, units} = 0.0049 \, V \, / \, unit \tag{12}$$

translating to an error margin of $\pm 5 \, units$

Due to these factors, the ultrasonic sensors, sonar 0, sonar 1 and sonar 2 recorded the same distance in different average voltage levels. Therefore each sensor was treated independently. However we observe slight fluctuations in range data values as a result of specular effects due to the transducer's position relative to the obstacle. This is because ultrasonic ranging sensors have high accuracy when the incident angle is less than half the beam angle [53], which is the angle around the acoustic axis where a target will be detected. The further from the perpendicular the incident angle is, specular reflection occurs resulting in falsely long readings [54].

In this study we did not consider a resultant size of the array $L = 2D$ of the combined two transducers of diameter $D = 1.5 \times 10^{-2}$ m but each transducer was

set to operate independent of the other with a beam width (Q) dependent on diameter (D). We also applied a maximum detection range of 3.0×10^{-1} m which we named minimum safe distance. In comparison with the sound beam pattern A in appendix L, we observe that the main lobe of the beam pattern has a diameter of 6.35×10^{-3} m at a maximum detection range of 9.14×10^{-1} m. Therefore, since a detection range of 3.0×10^{-1} m falls in this category of beam patterns for the LV-Max Sonar-EZ1 sensors, the acoustic beam in our case also had a diameter of approximately 6.35×10^{-3} m. It is clear from this that the incident angle of an incident sound pulse from a transducer must be too large for a neighboring transducer to receive unwanted echoes from it. This is because the main lobes of their acoustic beams respectively are at a separation distance of 9.99×10^{-2} m. This dictated the choice of distances d_l and d_r used in the navigation algorithm for a more accurate detection of the reflecting point on an obstacle surface. Due to this the angular orientation of an obstacle in the environment was obtained more accurately according to equation (8), as applied in the avoid loop.

The microprocessor's ADC presented the sonar range readings in words of 10 bits. As stated in section 4.2.5.1, the sensors convert range information to voltage values in a voltage range of 0 to 5 volts, which is the analogue input range. The 0 volt is therefore considered a logic LOW and 5 volts a logic HIGH. The fact that voltage values recorded within the voltage range are different from the HIGH and LOW characterizes digital signals.

The data on Tables 5.0, 5.1 and 5.2, are digital outputs of numbers ranging between 0 to 1023 called voltage levels or intervals depending on the distance recorded by a sensor. We take note that in the algorithm this is what is used to develop logic functions using comparison operators. The voltage levels representing a particular range for each sensor were averaged due to fluctuations, to minimize errors in positioning as dictated by comparison operators in the avoid and roll loops in the navigation algorithm as illustrated in section 4.4.2.

54

Table 5.0 are the sonar signatures representing voltage levels when $d_l = d_r$ table 5.1 when $d_l > d_r$ and 5.3 when $d_l < d_r$. From equation (8), since the obstacle width is taken as a constant, that is 0.1 m apart, the logic approach was restricted to d_l and d_r values only after the middle sonar 0 records a minimum safe distance reading. This enabled the robot to detect and avoid obstacles within the minimum safe distance before entering the obstacles cylinder which we defined as the danger zone as explained in section 4.4.2. We also take note that the boundaries utilized the short distance accuracy of sensors to keep the robot neither too close nor too far from the obstacles.

As explained in section 3.1, specular characteristics of flat obstacles in an indoor environment and the width of the ultrasonic beam, makes the real reflected point not to be located accurately on the transducer's line of sight. This is because the echo observed by the receiver is limited to the reflection from the foot of the perpendicular line of the obstacle drawn from the transducer. However as clearly shown in figure 4.12 with the adopted phase shift method, even when the transducers have a wide beam width, the resolution of the estimated reflection point is kept high since the robot could effectively detect and avoid obstacles in the indoor laboratory environment. This is because the adopted phase shift method gave a wide range of possibilities of directions of reflecting points, that is, a wide range of possible inclination angles of the obstacle's surface. The robot therefore was able to position itself more accurately in the indoor environment by detecting and avoiding obstacles.

CHAPTER SIX

CONCLUSION AND RECOMMENDATIONS

6.1 Conclusion

In this study, LV-Max Sonar-EZ1 ultrasonic sensors were used in the obstacle detection procedure and an algorithm developed using Arduino C version 11 provided the obstacle avoidance control procedure also referred to as the navigation algorithm. From the results presented in this study the following conclusions can be drawn:

1. The sensing style has an opposite property to conventional ultrasonic sensing. Conventional sensing has a feature that a high resolution is attained only when a single transducer has a narrow beam width. In the method used, we observed that even when the beam width is wide, considering more than one transducer in operation, the resolution of the estimated reflecting point is kept high. This provides a wide range of possible inclination angles of the obstacles surface because of the wide range of possible directions of the reflecting point. This is because flat indoor obstacle surfaces are like mirrors and therefore reflects the beam specularly.

2. While in motion, the robot could recognize corners and narrow openings. Rectangular corners give reflection for an ultrasonic beam even when a perpendicular wall does not exist. So, when in motion at a regulated speed considering the breaking distance to an obstacle, the robot builds a map of where surface elements are distributed representing the number of flat walls perpendicular to the robots position. Since at a corner the surface elements have various directions the robot recognizes that point as a corner.

56

3. When using a conventional ultrasonic sensor system, the robot knows its position error in the lateral direction in real-time by measuring the shortest distance to walls. With the adopted method, the robot can obtain "distance" and "inclination angle" of the obstacle at same time, and the robot is therefore able to revise both its position and orientation simultaneously. The robot usually needs to obtain two range values at different positions in order to obtain its orientation.

4. The adopted methodology minimized discrete angle errors in the reflecting direction relating to the ultrasonic wavelength. This was achieved by taking multiple reading as shown in tables 5.0, 5.1 and 5.2, and averaging them. The averaged values were implemented in avoid and roll loops of the navigation algorithm as shown in section 4.4.2. Due to this, the robot successfully avoided collision by maintaining a safe distance from the obstacles in the indoor environment.

6.2 Recommendations

The sonar configuration- the geometric relationship between transducers (transmitter/ receiver) and reflective features- considered in this study restricted us to only two ultrasonic sensors on the front panel of the robot and hence two range values. Despite being an effective method of determining the direction of reflecting point more accurately in comparison to conventional ultrasonic sensing, controlling the line-of-sight of the sensor to track the normal direction of the wall is the main challenge. This is because at a certain critical angle specular reflection takes place and all the signal is reflected away from the robot. In other words the obstacle is not detected since no echo is received. Further work could therefore involve either using a rotary method or a sonar ring configuration [55, 56, 57, 58] to minimize such an error when the transmitted signal is at an angle to an obstacle surface and no echo is received.

In the rotary approach, the system shall comprise of a transmitter and two receivers at the extreme ends on a single board supported by a stepper motor or two transducers at the extreme end of the board. The stepper motor's rotation is controlled by the robot's computer (microcontroller). This configuration can apply the phase shift approach by considering two range readings (from each transducer or receivers respectively) at an instant in the navigation algorithm.

The sonar ring configuration shall comprise of eight to twenty four sonar transducers evenly distributed around their periphery in a plane parallel to the base of the robot. This configuration can also apply the phase shift approach by considering data from pairs of transducers in the navigation algorithm.

Using these configurations tracking the normal direction of the wall is possible since at any position the transducers can receive echoes around a robots environment irrespective of the obstacle inclination. However, since the data obtained will be localized and heavily sampled a more detailed algorithm will be required to accurately position and navigate the robot system.

REFERENCES

1. Urick, R.,*Principles of Underwater Sound*, McGraw-Hill, New York, 1983

2. Goritov,A.N., Korikov,A.M., *Optimality in robot design and control*, Autom Remote Control 62, 1097-1103, 2001.

3. Pollack, J.B., Hornby,H., Lipson, Funes, P., *Computer creativity in the automatic design of robots*, Leonardo 36, 115-121, 2003.

4. Elfes, A., Bueno, S.S., Bergerman, M., de Paiva, Ramos, J.G., *Robotic airships for exploration of planetary bodies with an atmosphere*: *Autonomy challenges*, Autonom Robots 14, 147-164, 2003.

5. Hirose, S., Kuwahara, H., Wakabayashi, Y., Yoshika, N., *The mobility design concepts/ characteristics and ground testing of an offset-wheel rover vehicle*, Space Technol 17, 183-193, 1997.

6. Ito, T., Mousavi Jahan Abadi, M.S., *Agent-based material handling and inventory planning in warehouse*, J Intell Manuf 13, 201-210, 2002.

7. Letherwood,M.D., Gunter, D.D., *Ground vehicle modeling and simulation of military vehicles using high performance computing*, Paralllel Comput 27, 109-140, 2001.

8. McVea, D., Pearson, K., *Long-lasting memories of obstacles guide leg movements in the walking cat*. The Journal of Neuroscience, 2006.

9. Polaroid Corporation, Commercial Battery Division. *Ultrasonic Ranging System*, 1984.

10. http://www.eng.yale/ee-labs/morse/other/pos96ch4.pdf (7th March, 2012).

11. Simmons, J.A., Ferragamo, M.J., Moss, C.F., *Echo-delay resolution in sonar images of the big brown bat, Eptesicus focus*. In: National Academy of Science, Vol. 95, 12,647-12,652, 1998.

12. . Woodbury, N., Brubacher, M., Woodbury, J.R., *Noninvasive Tank Gauging with Frequency-Modulated Laser Ranging Sensors*, 27-31, September, 1993.

13. Kuc, R., Siegel,M., *Physically based simulationmodel for acoustic sensor robot navigation.* IEEE Trans. Pattern Anal. Mach. Intell. **9**, 766–778, 1987.

14. Moita, F., Feij˜ao, A., Nunes, U., de Almeida, A.T., *Modelling and calibration of an ultrasonic ranging system of a mobile robot.* In: Controlo 94, Lisbon 1994.

15. Randall, R.C., Michel, H.E., *Theoretical design issues of a multi-sensor doppler-tolerant ultrasonic system using pseudorandom codes.* In: The 2006 World Congress in Computer Science, Computer Engineering, and Applied Computing (ICAI'06), 628–634, Las Vegas, Nevada, USA ,2006.

16. Harris, K.D., Recce, M., *Experimental modelling of time-of-flight sonar,* Robot. Auton. Syst. **24**, 33–42, 1998.

17. Wilkes, D., Dudek, G., Jenkin, M., Milios, E., *Multi-transducer sonar interpretation,* Proceedings of the IEEE International Conference on Robotics and Automation, Atlanta, Goergia, USA, Vol. 2. 392-397, 1993.

18. Matthes, L., Elfes, A., *Integration of Sonar and Stereo Range Data using Grid-based Representation,* Proceedings of the IEEE International Conference on Robotics and Automation, Philadelphia, Pennsylvannia, USA, 727-733, 1988.

19. Peremans, H., Van Campenhout, J., *Tri-aural perception on a mobile robot,* Proceedings of the IEEE International Conference on Robotics and Automation, Atlanta, Georgia, USA, Vol. 1. 265-270, 1993.

20. Lawitzky, G., Feiten, W., Moller, M., *Sonar sensing for low-cost indoor mobility,* Robotics and Automation Systems, Vol. 14. 149-159, 1998.

21. Jorg, K.W., Markus, B., *Mobile Robot Sonar Sensing with Pseudo-Random Codes,* Proceedings of the IEEE International Conference on Robotics and Automation, Leuven, Belgium, 2807-2812, 1998.

22. Wirnitzer, B., Grimm, W., Schmidt, H., Klinnert, R., *Interference Cancelling in Ultrasonic Sensor Arrays by Stochastic Coding and*

Adaptive Filtering, IEEE International Conference on Intelligent Vehicles, Stuttgart, Germany, 1998.

23. Schmidt, H.,Klinnert,R., Grimm,W., *Sensorbasierte Umgebungserfassung durch Sensordatenfusion bei Verwendung Von Ultraschall-und Videobildsinalen*, Intelligente Serviceumgebungen, Shaker Verlag, Aachen, Germany. 35-45, 1999.

24. Barshen, B., Kuc, R., *Differentiating Sonar Reflections from Corners and Planes by Employing an Intelligent Sensor*, IEEE Trans. Pattern Anal. Mach. Intell., 12(6), 560-569, 1990.

25. Sabatini, A.M., *Active hearing for external imaging based on an ultrasonic transducer array*, In: IEEE/RSJ International Conference on Intelligent Robotic systems (IROS' 92), 829-836, 1992.

26. Kleeman, L., Kuc, R., *Mobile robot sonar for target localization and classification*, Int .J. Rob. Res. 14, 292-318, 1995.

27. Pires, G., Martins, N., Almeida, R., Moita, F., munes, U., de Almeida, A.T.: *Optimization of the tri-aural system, detection and identification of different reflectors*, In: Mechatronics 96 with M^2 VIP 96 Conference. Guimaraes, Portugal, 1996.

28. Hernandez, A., Urena, J., Garcia, J.J., Mazo, M., Hernanz, D., Derutin, J.P., Serot, J., *Ultrasonic ranging sensor using simultaneous emission from different transducers*, IEEE Trans. Ultrason. Ferroelectr. Freq. Control, 51(12), 1660-1670, 2004.

29. Araujo, E.G., Grupen, R.A., *Feature extraction for autonomous navigation using an active sonar head*, In: IEEE International Conference on Robotics and Automation (ICRA' 2000), 3823-3828, 2000.

30. Moita, F., Nunes, U., *Ultrasonic reflectors recognition with a first firing system*, In: SICICA 2003 5th IFAC International Symposium on Intelligent Components and Instruments for Control Applications, Averio, Portugal, 2003.

31. Borenstein, J., *The vector field histogram – fast obstacle avoidance for mobile robots*, IEEE Trans. Robot, Autom. ,7(3), 278-288, 1991.

32. Elfes, A., *Occupancy grids: a stochastic spatial representation for active robot perception*, In: 6th Conference on Uncertainty in AI, 1990.

33. Wijk, O., Christensen, H., *Triangulation- based fusion of sonar data with application in robot pose tracking*, IEEE Trans. Robot. Autom. 16, 740-752, 2000.

34. Feng, L., Borenstein, J., Everette, H.R., *Sensors and Methods for Autonomous Mobile Robot Positioning*, Technical Report UM-MEAM-94-21, December 1994.

35. Borenstein, J., *Control and kinematic design of multi-degree-of-freedom mobile robot with compliant linkage*, IEEE Transactions on Robotics and Automation, Vol. 11, No. 1. 21-35, February 1,1995.

36. Figueroa, F., Barbieri, E., *An Ultrasonic Ranging System for Structural Vibration Measurement*, IEEE Transactions on Instrumentation and Measurements, Vol. 40, No. 4. 764-769, August 1991.

37. Shraga, S., Johann, B., *Measurement of Angular Position of a Mobile Robot using Ultrasonic Sensors*, ANS Conference on Robotics and Remote Systems, Pittsburgh, PA, April 26-28, 1999.

38. Miller, G., Wagner, E., *An optical rangefinder for autonomous robot cart navigation*, In I. Cox and G. Wilfong, editors, Autonomous Robot Vehicles, 122-134. Springer-Verlag, 1990.

39. Cox, I.J., *An experiment in guidance and navigation of an autonomous robot vehicle*, IEEE Trans. Robotics and Automation, 7(3):193-204, 1991.

40. Tarassenko, L., Brownlow, M., Marshall, G., Tombs, J., Murray, A., *Real-time autonomous robot navigation using VLSI neural networks*, In R. Lippmann, J. Moody, and D. Touretzky, editors, Advances in Neural Information Processing Systems, volume 3, 422-428. Morgan Kaufmann, 1991.

41. Hinkel, R., Knieriemen, T., von Puttkamer, E., *Mobot-III an autonomous mobile robot for indoor applications*, In International Symposium and Exhibition on Robots, 489, Sydney, Australia, 1988.

42. Flynn, A.M., *Combining sonar and infrared sensors for mobile robot navigation*, International Journal of Robotics Research, 7(6), 1988.

43. Connell, J., *A Colony Architecture for an Arti⁻cial Creature.* PhD thesis, Massachusetts Institute of Technology, 1989.

44. Gough, P., de Roos, A., Cusdin, M., *Continuous transmission FM sonar with one octave bandwidth and no blind time*, In I. Cox and G. Wilfong, editors, Autonomous Robot Vehicles. Springer-Verlag, 1990.

45. Murray, D., Buxton, B., *Experiments in the Machine Interpretation of Visual Motion*, MIT Press, 1990.

46. Kuc, R., Di, Y., *Physically Based Simulation Model for Acoustic Sensor Robot Navigation, IEEE* Transactions on PAMI, 1987.

47. Kuc, R., Di, Y., *Intelligent Sensor Approach to Differentiating Sonar Reflections from Corners and Planes*, International Congress on intelligent Autonomous Systems Proceedings, Amsterdam, The Netherlands, 1986.

48. Letovsky, S., *Interpreting Range Data for a Mobile Robot*, CSCSI-SCEIO Proceedings, London, Ontario, 1984.

49. http://www.maxbotix.com/documents/MB1010-Datasheet.pdf (7th of March, 2012).

50. http://www.artmel.com/dyn/resouces/pro_documents/doc2549.pdf (7th of March, 2012).

51. www.ladyada.net/learn/arduino/ (7th of March, 2012).

52. Rodney, A.B., Anita, M.F., "Robot Being" NATO Workshop on Robotics and Biological Systems, Tuscany, Italy, July 1989.

53. Polaroid Corporation, *Polaroid Ultrasonic Ranging System Handbook*, Application Notes and Technical Papers, 1987.

54. Flynn, A.M., *Combining Sonar and Infrared Sensors for Mobile Robot Navigation*, International journal of Robotics Research, December 1988.

55. Leonard, J.J., Durrant-Whyte, H.F., *Direct Sonar Sensing for Mobile Robot Navigation*, Vol. SECS 175 of *The Kluwer Int. Series in Eng. and Comp. Sci.*, *Kluwer* Academic Publishers, Norwell, MA, 1992.

56. Peremans, H., Van Campenhout, J., Tri-aural perception on a mobile robot, In *Proc. IEEE Int. Conf. Robot. Automat.*, Vol. 1, 265–270, Atlanta, GA, May 1993.

57. Manyika, J., Durrant-Whyte, H.F., *Data Fusion and Sensor Management: A Decentralized Information-Theoretic Approach*, Ellis Horwood Series in Electrical and Electronic Engineering, 1994.

58. Crowley, J.L., Dynamic world modeling for an intelligent mobile robot using a rotating ultra-sonic ranging device, In *Proc. IEEE Int. Conf. Robot. Automat.*, Vol. 1, 128–135, St. Louis, MO, Mar. 1985.